JET–P(98)65

The JET Team
(presented by J Jacquinot)

Deuterium-Tritium Operation in Magnetic Confinement Experiments: Results and Underlying Physics

JET–P(98)65

Deuterium-Tritium Operation in Magnetic Confinement Experiments: Results and Underlying Physics

The JET Team (presented by J Jacquinot)

JET Joint Undertaking, Abingdon, Oxfordshire, OX14 3EA,

Preprint of a Paper to be submitted for publication in
Plasma Physics and Controlled Fusion

January 1999

ABSTRACT

A review of experimental results obtained in JET D-T plasmas is presented. In discussing the underlying physics, results previously obtained on TFTR are also taken into account. In JET, the maximum fusion power output (P_{fus}) of 16.1 MW has been obtained in an ELM-free hot-ion H-mode featuring an edge confinement barrier in a single-null divertor plasma with a $Q(\equiv P_{fus}/P_{in}) \approx 0.62$ where P_{in} is the total input power to torus. A steady-state H-mode discharge, with plasma shape and safety factor q similar to that of ITER, produced 4 MW for 5s (22 MJ). The steady-state results extrapolate well to ignition with ITER parameters using the normalized plasma pressure (β_N) achieved on JET. Also, the Advanced Tokamak regime using optimized magnetic shear configuration featuring an internal transport barrier produced 8.2 MW of fusion power. With regards to reactor physics issues, a clear identification of electron heating by fusion born alpha particles has been made both in JET and TFTR. The JET experiments show that the H-mode threshold power has approximately an inverse isotopic mass dependence and that it does not depend on the method of auxiliary heating. The global energy confinement time in the TFTR D-T supershot regime scales as $\sim A^{0.85}$ but in the JET H-modes, it is found to be practically independent of isotopic mass ($\sim A^{0.03\pm0.2}$) where A is the atomic mass of the hydrogenic species. In JET, the plasma core and the edge appear to have different underlying confinement physics, the former follows the gyro-Bohm transport ($\sim A^{-0.2}$) model whereas the edge pedestal energy scales as $\sim A^{0.5\pm0.2}$. The maximum edge pressure in H-modes is analyzed in relation to the ion poloidal Larmor radius at the edge. The fast ions driven by NBI or ICRH could play an important role in setting the width of the edge pedestal. The thermal ELMy H-mode confinement both in D or T gas fuelled plasmas decreases significantly when the plasma density exceeds 0.75 of the Greenwald (n_{GW}) limit and the maximum density achieved is $0.85n_{GW}$. The ICRH scenarios for a reactor have been evaluated. For example, He3-minority in 50:50 D:T and tritium dominated plasmas showed strong bulk ion heating leading to ion temperatures up to 13 keV with ICRH alone. Deuterium minority ion cyclotron heating in tritium plasmas at a power level of 6 MW produced a steady-state record values of $Q \approx 0.22$ for more than 2.5s. Finally, the on-site closed-cycle tritium reprocessing plant and remote handling tools at JET have been used routinely and provided an integrated demonstration of safe and reliable operations of a tokamak device in reactor-relevant conditions.

1. INTRODUCTION.

In controlled thermonuclear fusion research, two main-line approaches, magnetic and inertial confinement, have been pursued. One of the most successful concepts in magnetic fusion is the tokamak confinement scheme which has attained plasma parameters close to those that are needed in a fusion reactor. Most fusion devices carry out experiments in hydrogen or deuterium, simulating operations with the fusion fuel which is roughly a balanced mixture of deuterium (D) and tritium (T). Nevertheless, two of the world's largest tokamaks, the JET European Torus (JET)

[1] and the Tokamak Fusion Test Reactor (TFTR) [2] were planned to operate with tritium and, indeed, have carried out full-fledged D-T experiments. These D-T experiments impose stringent requirements on site-facilities which must tolerate a significant level of machine activation and accommodate the safe handling of radioactive gas.

The very first tritium experiments, the Preliminary Tritium Experiments (PTE), were carried out at JET in 1991 [3]. In these experiments, only two discharges with 11% tritium in deuterium plasmas (a mixture far away from the optimum 50:50 D-T) were made which produced a fusion power 1.7 MW and a $Q(\equiv P_{fus}/P_{in})\approx 0.12$. From 1993-1996, an extensive campaign of high power D-T experiments was conducted in TFTR with a wider range of D-T mixtures. Using the optimum 50:50 D:T mixture, a fusion power output of 10.7 MW and a fusion $Q\approx 0.27$ [4] was obtained in the so-called Supershot regime in a circular limiter plasma. An excellent review of these results can be found in [5]. In 1997, a new series of D-T experiments at JET (DTE1), a maximum fusion power output of 16.1 MW [6] and a $Q\approx 0.62$ have been obtained in the ELM-free hot-ion H-mode in a single-null divertor plasma. An overview of JET D-T results are given in [6,7].

This progress in magnetic confinement based tokamak devices has generated Engineering Design Activities (EDA) of the International Thermonuclear Experimental Reactor (ITER) [8]. The JET device has the capability to match the proposed ITER geometry, safety factor q and most of the key physics dimensionless parameters such as β and ν^*. The largest deviation is in the normalized Larmor radius ρ^* which is a factor of 3 to 5 higher in JET than in ITER. The parameter ρ^* is a key parameter in the prediction of reactor performance and it has been varied systematically in JET experiments in order to provide the basis for extrapolation to ITER. Here, ρ^* ($\equiv \rho_i/a$), ν^* ($\equiv \nu_e a/v_{th}$) and β ($\equiv 2\mu_0 \langle p \rangle / B_\varphi^2$) where ρ_i is the ion Larmor radius, a is the minor radius in the mid-plane, ν_e is the electron-ion collision frequency, v_{th} is the ion thermal velocity, $\langle p \rangle$ is the average plasma pressure and B_φ is the toroidal field.

There are three main objectives of the D-T experiments: (i) a demonstration of significant fusion power production in physics conditions relevant to reactor applications, (ii) a study of ITER physics issues such as α-particle heating, confinement and plasma stability, scaling of isotopic mass dependence of energy confinement and H-mode threshold and (iii) a demonstration of reactor-relevant technologies such as closed-loop tritium gas reprocessing and remote handling of major tokamak in-vessel assemblies.

A number of plasma modes of operation (including the L-mode) have been investigated in JET and TFTR in D-T plasmas for the production of significant fusion power. Some of these regimes are: ELM-free hot-ion H-mode [6], supershot regime [4], high-ℓ_i mode [9] and optimised magnetic shear regime of operation [10,11]. Also, studies of steady-state operation using ELMy H-modes, the ITER reference scenario, have been made at JET.

Experiments performed in the area of reactor physics issues have been focused on (a) alpha-particle heating studies [12,13], (b) excitation and study of Toroidal Alfven Eigenmodes

[14,15] which are plasma instabilities that could occur in burning plasmas when α-particle velocities match the Alfven speed (c) the isotope scaling of H-mode threshold power [16], energy confinement [17,18], edge localized modes (ELMs) and pressure pedestal [19] together with an insight into core and edge transport physics, (d) confinement at high density including the density limits in H-modes [20] and (e) ion cyclotron resonance heating (ICRH) experiments including the demonstration of reactor scenarios of tritium second harmonic heating, D-minority heating in tritium plasmas [21,22] and benchmarking of ICRH codes for reactor applications [23].

Fusion technology issues consist in tritium fuel cycle, remote handling and safety of operation. For JET experiments, 20 g of tritium were used. This allowed a significant number of D-T shots during a period lasting typically 3-4 days. The exhaust gases were then collected and reprocessed (usually in 3-4 days) by the on-site closed-circuit Active Gas Handling System (AGHS) [24] for subsequent experiments. The total neutron production in the DTE1 experiments was limited to 2.5×10^{20} neutrons in order to permit manned in-vessel intervention with low radio active exposure after about 18 months. It was not necessary, however, to wait for such a period to make all the in-vessel modifications required by the JET programme because the remote handling tools [25] were successfully implemented to remove the JET MkIIAP [26] divertor tile carriers and replace them with new elements to establish the new MkIIGB divertor [26] configuration. In TFTR, the total number of neutrons produced during the 1993-1996 period of operation was 4.8×10^{20} neutrons whereas in the PTE experiments in 1991 in JET, 1.5×10^{18} neutrons were produced. The above JET and TFTR D-T experimental campaigns were conducted safely and any tritium discharges to the environment were at least an order of magnitude below the maximum levels imposed by the local regulatory authorities.

In this paper, we present a review of JET experimental results and the underlying physics of JET and TFTR tokamak D-T plasmas. In section 2, we briefly outline the experimental set-up used in the D-T experiments. Section 3 deals with the various modes of operation and fusion performance in D-T plasmas and an extrapolation to ITER which is based on steady-state experiments at JET. In section 4, we discuss the results relating to reactor physics issues. The fusion technology aspects are presented in section 5 and finally, the discussion and conclusions of the paper are contained in section 6.

2. EXPERIMENTAL SET-UP.

The main plasma parameters of JET and TFTR are given in Table 1 which also includes parameters used for the Engineering Design Activities (EDA) of ITER, for comparison. The JET device features a single-null divertor configuration with elongated plasmas whereas TFTR used a circular plasma limited by a limiter on the inner wall (see Fig.1). In both devices, outboard poloidal limiters are used to protect the ICRH antennas located on the low-field side. Some of the JET in-vessel components are shown in Fig. 1. These include ICRH antennas, a cryo-pump

Table 1: JET, TFTR and ITER Parameters

Parameter	Units	JET	TFTR	ITER/EDA
Typical major radius	m	2.85	2.6	8.1
Typical minor radius	m	0.95	0.9	3
Plasma elongation		1.8	1	1.6
Toroidal magnetic field on axis	T	3.8	5.9	5.7
Plasma current	MA	6	3	21
Flat top pulse length	s	0 – 60	0-5	1000
Transformer flux	Wb	42		608
NBI power	MW	22	40	100MW with several methods
ICRH power	MW	17	11	
LHCD power	MW	10	—	
Power exhaust		SN(D) Divertor	Limiter	SN(D)Divertor

SN(D)= single null X-point down.

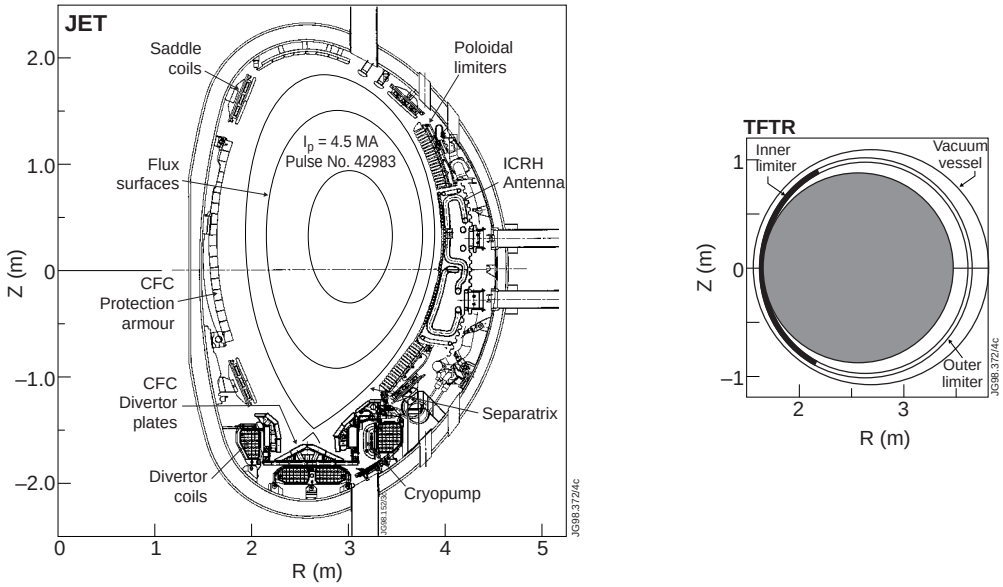

FIG. 1. Poloidal cross sections of JET and TFTR tokamaks. Also, shown are the four divertor coils, MkIIaP divertor target plates, the cryopump, an ICRH antenna, a poloidal limiter and saddle coils inside the JET vacuum vessel. Plasma flux surfaces together with the separatrix of a 4.5 MA discharge are also illustrated.

in the divertor region, shaped divertor tiles made out of carbon composite fibre (CFC), in-vessel divertor coils generating the X-point divertor configuration and saddle coils for error field and Alfven eigenmode excitation studies. The neutral beam injection (NBI) and ion-cyclotron resonance heating (ICRH) are the main heating systems used in JET and TFTR. The TFTR NBI

heating system [27] consists of four beam lines each with three positive ion sources. The ion sources can operate in deuterium or tritium with a maximum voltage of 120 kV delivering a maximum of 40 MW into a D-T plasma. The JET NBI system [28] is composed of two beam boxes with eight positive ion sources each. One of them has been used to deliver up to 100% tritium beams injecting about 11 MW of beam power at 155 kV for up to 5 s. The other box is used for deuterium beam injection delivering up to 12 MW at 80 kV. The JET ICRH [29] system couples up to 16 MW of power via four antennas distributed around the torus. The ICRH antennas are equipped with Faraday shields made out of beryllium. Each antenna has four straps which can be phased independently. The system has been operated at various frequencies (23-56 MHz) over the full bandwidth of the system. The TFTR ICRF system [30] uses four antennas with two straps each and can operate at 30, 43 and 64 MHz delivering a maximum power of 11 MW.

In view of the limited neutron budget during the JET DTE1 campaign, automatic feedback real-time control systems have been implemented so that if the desired performance or a desired plasma parameter is not achieved at the expected time during a discharge, the plasma shot is terminated with a soft landing. Also, various combinations of plasma parameters can be maintained at a programmed level by a system controlling, in real time, a number of auxiliaries such as neutral beam injection, ICRH and lower hybrid current drive (LHCD) power [31] thus improving reliability of discharges. The ICRH and/or NBI power delivered to the plasma was routinely controlled with precision using digital real-time techniques.

The tritium gas in JET was either injected directly to the torus via a gas valve or supplied to the NB box which then injected a small fraction of it to the torus via the neutral energetic tritium beams. The remaining gas was trapped by the NB cryo-pumps which was retrieved by regeneration and then reprocessed by the AGHS plant for reuse. In all about 100 g of tritium was used out which 27 g was injected in the main vessel and 73 g in the NBI box. About 40% of the tritium injected in the torus remained trapped transiently (over days and weeks) in the vessel and only about 1mg was consumed in the fusion reactions. More than 80% of tritium concentration in Ohmic plasmas could be obtained with about ten 100% tritium gas fueled discharges. With significant supplementary heating (>10MW), additional tritium loading discharges were required to maintain a high tritium concentration. Glow discharge is used for wall conditioning after a vent and beryllium evaporation is carried out when needed for gettering purposes (less than once a day). The tokamak operation is carried out with vessel walls at 320°C. As mentioned above, a significant fraction of the tritium injected in the torus remained trapped in the first wall components (~11 g). After the DTE1 campaign, it was possible to remove 5 g of tritium using various plasma cleaning techniques. However, an appreciable amount (6 g) still remained trapped. A mechanism for significant tritium retention is co-deposition forming flaking films in cold regions of the divertor structure. The flakes are not subjected to plasma bombardment. A considerable amount of flakes were observed in the cold part of the divertor structure. After the remote

divertor tile exchange and vacuum cleaning the flakes, about 1g of tritium has been left in the vessel.

The standard JET diagnostics for electron density (n_e), electron temperature (T_e), ion temperature (T_i), effective charge (Z_{eff}) have been discussed elsewhere [32]. For tritium compatibility and safety, modifications had to be made to the installed diagnostics. These include double containment vacuum feed-throughs with 500 mBar neon gas in the interspaces, exhaust from diagnostics vacuum systems sent to AGHS plant when necessary, extra neutron shielding, radiation hardened video cameras and heated optical fibres to recover from radiation damage. The most notable new diagnostics in DTE1 were the 14 MeV neutron energy resolved tomography and the measurements of the tritium concentration in the core and edge of the plasma as well as in gaseous exhaust after a discharge using residual gas analysis (RGA) and ion chamber measurements. The tritium concentration in the core was estimated from neutron emission rates and active Balmer-α charge exchange measurements. In the plasma region 20-40cm inside the separatrix, the tritium concentration was derived from neutral particle analysis (NPA) by electrostatic deflection and time of flight techniques. Near the separatrix, Balmer emission spectroscopy was used. Below divertor tiles, Balmer emission from Penning discharge gauges was implemented [33].

3. MODES OF OPERATION AND FUSION PERFORMANCE

In this section, we first outline the general features of different enhanced energy confinement modes of operation and then discuss the fusion performance obtained in some of these regimes in TFTR and JET D-T plasmas including steady-state discharges. Based on the latter, the performance is extrapolated to ITER-like plasma parameters.

3.1 General Features:

Energy confinement in tokamaks is generally observed to be much worse than that predicted by the neoclassical theory of collisional diffusion. Energy transport across lines of forces can vary greatly with modes of operation (see Table 2). Sudden bifurcations between the regimes is often observed. The principal confinement modes are illustrated schematically in Fig. 2 by indicating plasma temperature profiles for each regime.

L-Mode.

The L-mode ('L' for low confinement) is the most common mode of tokamak operation. The anomalous transport is governed by plasma instabilities with a radial scale length of the turbulence commensurate with the plasma minor radius. When the safety factor $q>1$, the sawtooth instability occurs in the central region of the plasma which periodically flattens the temperature profile as indicated in Fig. 2.

Table 2: Characteristics of Tokamak Regimes

Tokamak Modes	Duration	Sawteeth	Core Transport	IT-B	Edge Confinement Barrier	SOL Limiter Divertor
L-mode	CW	yes	turbulence scale ~ a	no	no	
Supershot	transient so far	none due to fast ion stabilisation	reduced	no	no	low recycling: Lithium conditioning
H-mode (ITER ref)	CW	yes	reduced	no	yes, above a power threshold	ELMs
Hot-ion H-mode	transient so far	none due to fast ion stabilisation	strong reduction	no	yes no elms	low recycling
Advanced Tokamak	CW need current Drive for Ip control	none due to q > 0	reduced to neo-classical χ_i	yes	possible	
Radiative improved (not seen in JET yet)	CW	yes	reduced	no	possible	seed impurities are added

H-Mode.

An enhanced confinement regime known as H-mode was discovered in the ASDEX tokamak [34] operating with a divertor plasma. In this mode, a transport barrier is established at the edge which improves the energy confinement. The stored energy is increased not only from the contribution of the edge pressure pedestal but also from an improvement of the core plasma. The H-mode is accompanied by ELMs which eject particles and energy from the edge and reduce the edge pedestal periodically (see Fig. 2). Though ELMs lead to some reduction in the confinement, they prevent the uncontrolled build up of density, impurity and helium ash. This regime forms the present basis for the steady-state tokamak reactor operation. It has been used in JET D-T experiments to produce 4 MW of fusion power for more than 5 s.

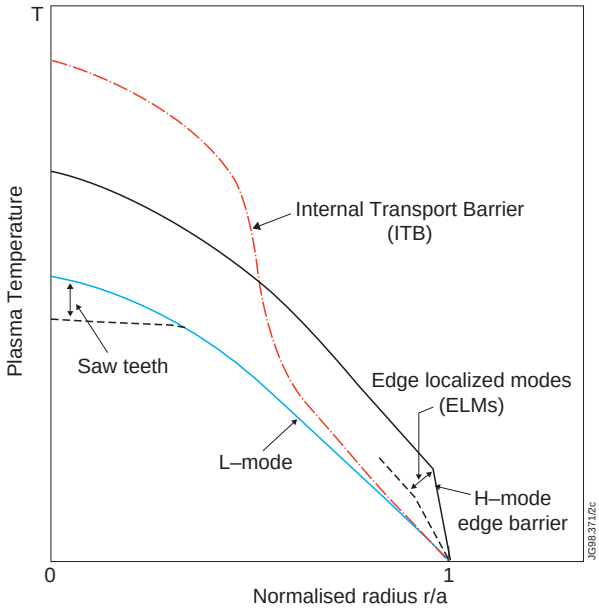

FIG. 2. Tokamak temperature profiles are shown schematically for a number of modes of operation. Sawteeth flatten the central electron temperature profile periodically whereas the ELMs degrade the edge pedestal.

ELM-free Hot-Ion H-mode.

This mode of operation [35], though transient, is one of the highest performance operating regimes in JET divertor discharges. It is obtained by strong neutral beam heating of a low density target plasma. Central NB power deposition and central fuelling produces a moderately peaked density profile and high ion temperatures such that T_{i0}/T_{e0} ~ 2-2.5. Long ELM-free periods (~2 s) are produced by conditioning the first-wall to achieve low recycling in a discharge with high triangularity (~0.25) and a high flux expansion in the divertor. The high performance is generally terminated by an MHD event [36] involving either (i) a sawtooth or other internal MHD phenomena occurring in the central region, (ii) 'outer modes' occurring in the body of the plasma or (iii) 'giant' ELMs at the plasma edge.

Optimised Shear Regime.

Enhanced performance is also obtained when the plasma current density profile meets certain criteria. This mode is also referred to as the Advanced Tokamak regime featuring a potentially 'well aligned' bootstrap current-density profile consistent with full steady-state operation in a reactor [10,11] . In this regime, the core transport is reduced by operation in weak or slightly negative magnetic shear in the core region (weakly hollow current-density profiles) and ensuring that q>1 every where in the plasma. Such discharges were first obtained in JET experiments with deep pellet injection and the mode was termed as PEP mode [37]. More recently, the magnetic-shear profile has been optimized by controlling the current diffusion during the current ramp-up phase of the discharge together with active current profile intervention by the LHCD power. MHD instabilities like ballooning, resistive tearing and internal MHD modes are stabilized provided that low rational values of q are avoided. Shear of plasma rotation has also been shown by theory to stabilize microinstabilities involved in anomalous transport. In such a situation, an internal transport barrier (ITB) can be established resulting in a steep temperature gradient in the core region [10]. In some instances, this ITB regime can be combined with the edge barrier of the H-mode enhancing the performance even further. The ITB has been established in D-T discharges in TFTR [11], JT60-U [38] and JET [10], the latter producing 8 MW of fusion power.

Supershot Regime.

In limiter discharges in TFTR, another enhanced confinement scheme (see Table 2) the so-called 'supershot' [39] regime was demonstrated where the core transport is substantially reduced compared with L-mode by extensively conditioning the limiters (including lithium coating) to decrease the influx of deuterium and carbon from limiters and the vessel wall. Supershot discharges are characterized by peaked density profiles, high ion temperatures (T_{i0}/T_{e0} ~ 2-4), high T_i at the edge and strong beam particle fuelling [5]. The reduction in transport [40] is associated with the suppression of ion-temperature gradient driven modes due to large values of plasma rotational shear induced by the strong particle fuelling and ion heating sources provided

by the beams. The high performance is terminated by β-limits and/or increased influx of carbon/ deuterium from the limiters. In this mode of operation 10.7 MW of fusion power has been produced in TFTR.

High-ℓ_i Mode.

In another regime in TFTR, the so-called high-ℓ_i discharges were used in which the current-density profile is peaked increasing the internal inductance of the plasmas, for example, by rapidly decreasing the plasma current. Other techniques have also been used to produce high-ℓ_i discharges [41]. The high performance of these discharges is limited by the occurrence of carbon blooms at high heating powers. High performance has been obtained in such a regime in JT60-U and TFTR. The maximum fusion power of 8.7 MW was obtained in high-ℓ_i D-T discharges in TFTR.

Radiative Improved (RI) Mode.

Radiatively improved confinement was first achieved on ISX and developed to a high density regime by TEXTOR [42]. Edge radiation cooling is obtained using silicon or neon as the radiating impurity. Radiating away a significant part of the power would be an advantage in a reactor from the power exhaust point of view. This mode of operation is known as RI-mode and has also been successfully attempted in other machines such as DIII-D, Tore-Supra, ASDEX-Upgrade and TFTR [43]. The RI-mode is characterized by high edge radiation (up to 85%) due to heavy seeded impurity ions and the core energy confinement is improved (by a factor of ~2) over the L-mode. Qualitatively, the presence of heavier ions in the plasma periphery decreases the level of turbulence at the edge [44] which in turn also improves the confinement in the core. In this regime, peaked density profiles are produced and there is no apparent accumulation of impurities in the centre. The current density profiles are also peaked similar to the above high-ℓ_i discharges which have a potential problem of bootstrap alignability for steady-state operation of a reactor. This mode of operation has not yet been attempted in D-T plasmas.

3.2 Fusion Performance.

3.2.1 ELM-free Hot-Ion H-Mode.

The highest peak fusion performance in JET has been obtained in the ELM-free hot-ion H-mode. To achieve the maximum fusion power output, specific D-T experiments were conducted [45] to determine the relative contributions of the NB fuelling and wall recycling to the plasma mix so that near optimum D-T mixture could be obtained during high fusion yield experiments. It was found that with D-T operation in MkIIAP [26] divertor, the sum of the gas supplied from the wall recycling, the target plasma and the direct gas injection contributes twice as much to the D-T mixture in the plasma as the NB fuelling. Therefore, the walls were loaded using 3-5 Ohmic or ICRF heated discharges with the gas fuelling adjusted until the D-T plasma mix was close to 50:50. In Fig. 3, we present time traces of the record discharge at a toroidal field (B_ϕ) of 3.6T

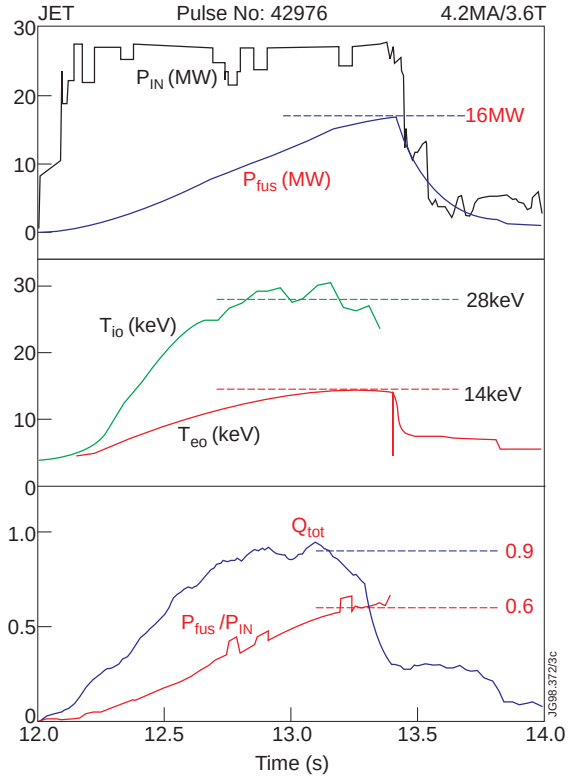

FIG. 3. Time traces of the highest performance JET D-T hot-ion H-mode discharge producing a record fusion power output of 16 MW and a $Q=P_{fus}/P_{in}$ = 0.62.

and plasma current (I_p) of 4.2 MA that produced 16.1 MW of fusion power. The discharge was heated with the maximum available NB power of 22.3 MW and an ICRH power of 3.1 MW. The occurrence of a sawtooth during the high performance phase was avoided by a fine adjustment of the gas feed. The central ion (T_{i0}) and electron (T_{e0}) temperatures reached 28 and 14 keV respectively. The high performance is terminated with the occurrence of a giant ELM which is provoked by steepening edge gradients as the central ion temperature rises. The maximum value of the fusion power amplification factor ($Q\equiv P_{fus}/P_{in}$) is 0.62 as indicated in Fig. 3 where P_{in} refers to the total input power into the torus including Ohmic, ICRH and NBI powers. The above definition of Q provides a simple measure of fusion performance of steady-state discharges but in discharges where there is a significant variation of stored energy (W) or heating power (P_{in}), several other definitions of Q have been used by the fusion community which may differ from one research group to another [5]. In order to identify the fusion power balance during the transient phase of the above discharge, we define $Q_{tot}\equiv P_{fus}/P_{loss}$ where $P_{loss} = P_{in}$-dW/dt and we include the contributions of beam-beam, beam-thermal and thermal fusion reactions in P_{fus}. In this discharge, Q_{tot} is maintained at a value of 0.9±0.17 during 0.3 s as indicated in Fig. 3.

3.2.2 Neutron Calculation by TRANSP Code.

Calculations of neutron production are performed by the TRANSP data analysis code [46] which uses the measured plasma parameters and their profiles to calculate the neutron source rates from thermal, beam-thermal and beam-beam fusion reactions. Good agreement is found between the total measured and calculated neutron source rates for the highest fusion performances in a Supershot discharge in TFTR (P_{fus}=10.7 MW) and a hot-ion H-mode discharge in JET (P_{fus}=16.1MW) shown in Fig. 4 and 5 respectively. This agreement is a good test of the overall consistency of measured plasma parameters. A comparison of the subdivision between the three sources of fusion neutrons in the two shots of TFTR and JET shows that, in JET, the neutrons of thermal origin constitute the main source whilst in the TFTR shot, the beam-thermal neutrons exceed significantly those of thermal origin and that the beam-beam contribution is about 15%. This reflects the higher plasma confinement time obtained in JET.

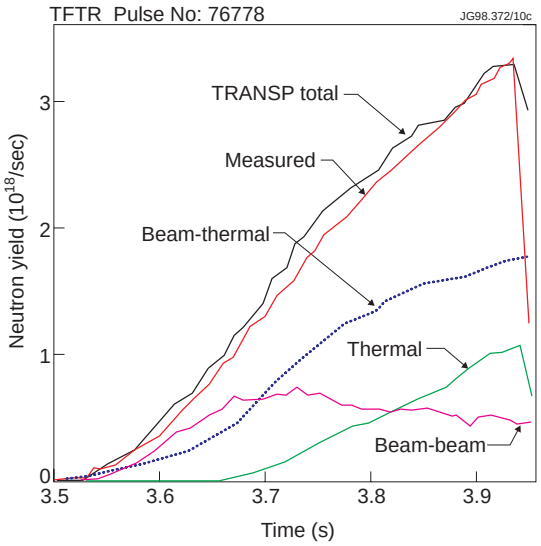

FIG. 4. Time evolution of the observed total neutron yield is compared with a simulation from the TRANSP code for the highest (10.7 MW) fusion power output shot of TFTR. Also shown are the thermal, beam-thermal and beam-beam contributions to the neutron yield as predicted by the code.

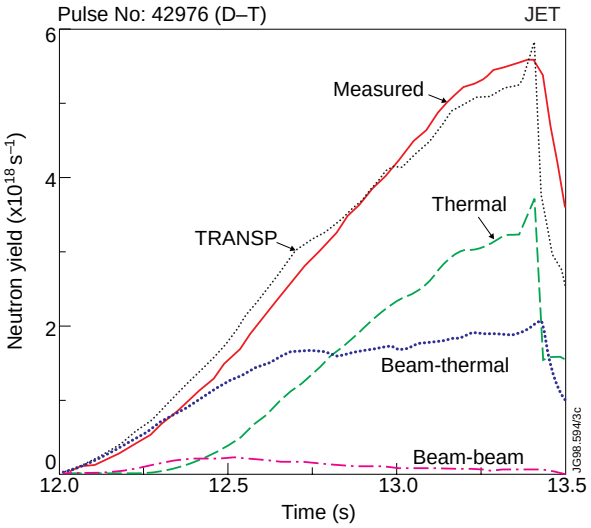

FIG. 5. Time evolution of the observed total neutron yield compared with a provisional simulation (run Y905) from the TRANSP code for the highest (16.1 MW) fusion power output shot of JET shown in Fig. 3. Also shown are the thermal, beam-thermal and beam-beam contributions to the neutron yield as predicted by the code. This simulation is presently undergoing further checks and verifications of ion temperature and effective charge.

3.2.3 Steady-State ELMy H-Mode.

High performance in steady-state ELMy H-mode discharges has been obtained in JET under ITER-like conditions with the key physics dimensionless parameters such as β, ν* and q being fixed close to their ITER value. Central electron and ion temperatures were roughly equal as expected in future ignited plasmas. However, due to the lack of input power, in some discharges, β-values could fall short of the one required in ITER. The time evolution of one such high performance steady-state ELMy H-mode discharge at 3.8T/3.8MA in a 50:50 D:T plasma with a total input power of 22 MW (predominantly NBI-power) is illustrated in Fig. 6. The discharge has type I ELMs throughout and the stored energy is practically stationary for 3.5 s which is about 8 energy confinement times. The duration of the discharge is only limited by the duration of NBI at full power. Fusion power output which reached a steady-state value of more than 4MW is also shown. The steady-state Q ($Q \equiv P_{fus}/P_{in}$) value is 0.18 over 3.5 s of the discharge. Integrated over

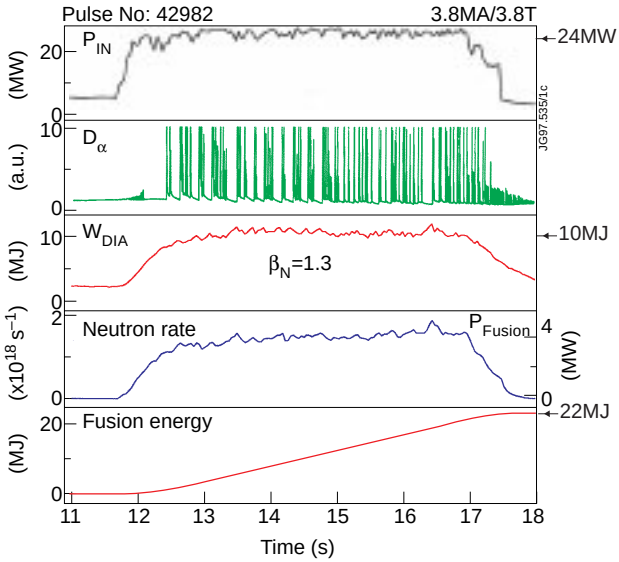

FIG. 6. Time traces of a near steady-state high performance JET discharge at 3.8T/3.8MA in 50:50 D:T mixture with an input power (P_{in}) of 24 MW. Diamagnetic stored energy (W_{DIA}) reached 10.5 MJ, fusion power output (P_{FUS}) and total Q ($\equiv P_{FUS}/P_{in}$) are 4.1 MW and 0.18 respectively. ELMs are shown by the D_α-signal.

the entire pulse, the fusion energy reached a value of 22 MJ which is a world record. The central line averaged density is about $7x10^{19}$ m^{-3} and droops a little towards the end of the high performance phase of the discharge. At such a high density, due to the short electron-ion equilibration time, the electron and ion temperatures are roughly equal at about 8.5 keV. Another ELMy H-mode steady-state discharge [47] at a lower value of q_{95}= 2.8 (3.8 T/4.5 MA) was found to have good energy confinement (H97 ≈ 0.95) with respect to ITERH-97P-scaling [48]. These results obtained at lower q_{95} (≡q at the normalized radius r/a=0.95) in D-T plasmas are of significant interest for ITER for providing larger ignition margins. These results are further supported by the ITER similarity experiments in deuterium plasmas [47].

3.2.4 Steady-State Fusion Performance with ICRH.

A high performance steady state discharge (3.7 T/3.7 MA) was also obtained by ICRF heating alone [22] with D-minority heating in a tritium plasma (9:91 D:T mixture). Despite the D:T mixture being far away from 50:50, a fusion power output of 1.6 MW was obtained with an input ICRH (f=f_{CD}=28 MHz) power of 6 MW only as shown in Fig. 7. In this discharge, the plasma density and the minority ion concentration was such that the average deuterium tail energy was about 120 keV (close to the peak of D-T fusion cross section). In this discharge, the neutrons thus produced are predominantly of non-thermal origin. The steady-state (for about 2.7 s) Q value is about 0.22 (a record value in steady-state conditions) whereas the central ion and electron temperatures are both at 7 keV. The neutron yield could be well reproduced by the PION code and confirms the non-thermal origin of these neutrons [23]. The PION code uses a sawtooth redistribution model but otherwise has no free parameters.

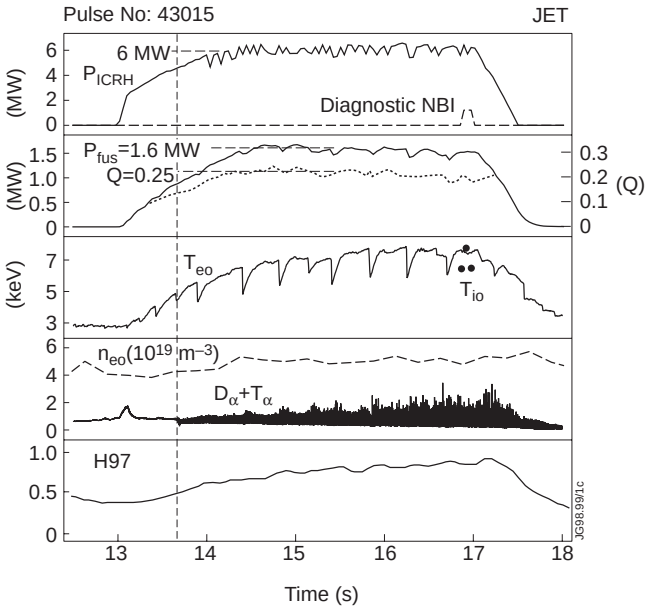

FIG. 7. Time traces of a near steady-state JET discharge at 3.8T/3.8MA in 9:91 D:T mixture heated by ICRH in D-minority in tritium with an input power of 6 MW. Fusion power output is 1.6 MW making a record Q=0.22 for a duration of more than 2.5 s. Here, H97 represents the ITERH97-Py H-mode confinement factor which is above the value required by ITER.

3.2.5 Optimised Shear Discharge.

A flat or hollow current-density profile with weak or negative values of the magnetic-shear s (s≡r/q(dq/dr)) is one of the conditions necessary to establish an internal transport barrier (ITB) that reduces the transport in the core close to neo-classical values. Strong core fuelling and/or heating is also found to be necessary for the formation of the ITB. The reduction in transport is often linked to the **E**x**B** shear stabilisation of the turbulence. This regime, called "optimized shear", requires careful preparation of the current-density profile of the target plasma. First, a

fast current ramp and early plasma expansion to full aperture is made during which the LHCD power is applied to produce a low inductance plasma at start-up. This is followed by ICRH pre-electron-heating to delay the inward diffusion of plasma current (see Fig. 8). When the size of the q=2 surface is about 1/3 of the plasma radius, full heating power is applied (~16-18 MW of NB and 6MW of ICRH) on a low target density plasma and the current ramp is continued. An ITB forms and the plasma profiles become very peaked (see Fig. 9). The good core confinement delays the power flux through the separatrix thus avoiding the trigger of an H-mode (see section 4.2) and keeps the plasma edge in the L-mode. The continued increase of the plasma current also increases significantly the H-mode power threshold. As β_N increases with time, the ITB expands radially outward to about 2/3 of the plasma radius and the pressure profile becomes less peaked. In this way, the plasma can remain within the ideal MHD stability β-limit for most of the high power heating phase [49] and major disruptions can be avoided. When the power flux through the separatrix exceeds a level such that it is above the H-mode threshold, the high performance

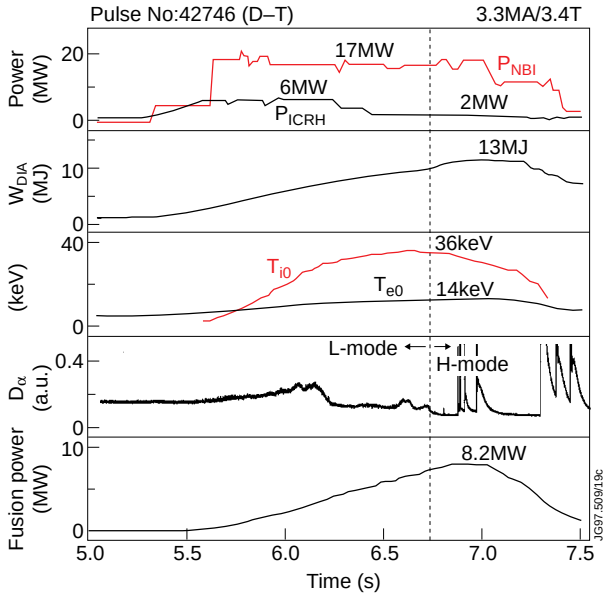

FIG. 8. Time traces of an optimised shear discharge in JET where the fusion power output reached 8.2 MW. The performance degrades at the appearance of ELMs. Central ion and electron temperatures reached 36 and 14 keV respectively.

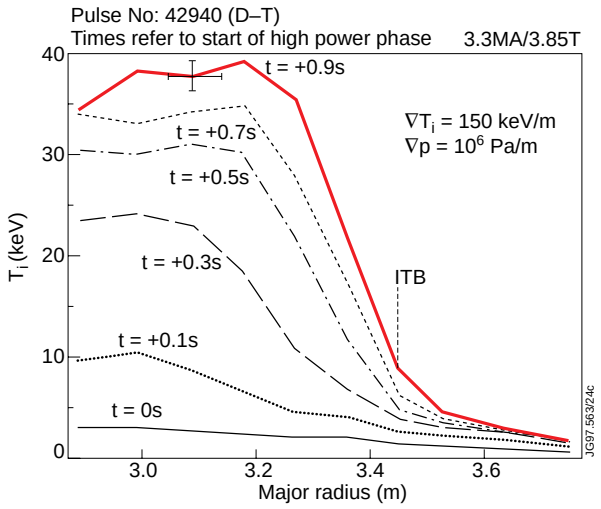

FIG. 9 (a) Ion temperature profiles measured by charge-exchange recombination spectroscopy for a number of time slices during an optimised shear discharge in D-T plasmas in JET. The time (t) parameter refers to the start of the high power phase. An internal transport barrier is triggered at t=0.3 s.

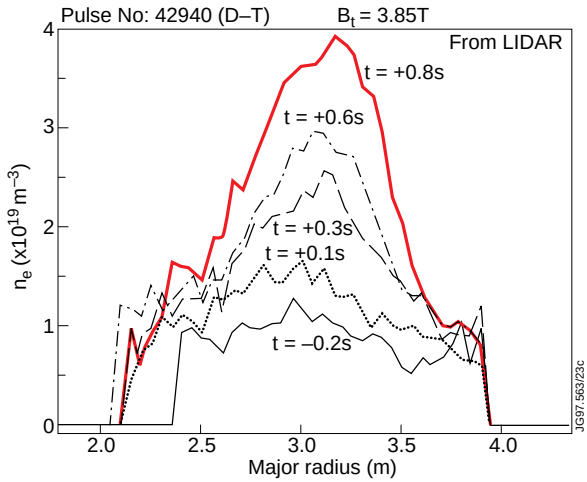

FIG. 9 (b) Electron density profiles measured by LIDAR diagnostics for a number of time slices during an optimised shear discharge in D-T plasmas in JET. The time (t) parameter refers to the start of the high power phase.

phase is often terminated by the occurrence of a giant ELM. In D-T plasmas, the H-mode threshold power is about 20% lower (see section 4.2) and therefore the H-mode was found to be triggered earlier than in D-D plasmas. This prevented the use of discharges developed in D-D to D-T directly. Optimization had to be done in D-T itself which was severely limited by neutron economy.

As shown in Fig. 8, in the best ITB discharge in D-T plasma, a fusion power of 8.2 MW was obtained. The maximum diamagnetic stored energy was 13 MJ. The central ion (T_{i0}) and electron (T_{e0}) temperatures reached 36 and 14 keV respectively. Such high ion temperatures are the result of combined effect of ICRH and NBI. The fundamental minority hydrogen heating also permits the ICRH power to be damped at second harmonic of deuterium and third harmonic of tritium thus depositing a part of the power (~3-15%) on the beam ions [50]. The expansion of the transport barrier can be seen from ion temperature profiles shown in Fig. 9 (a) at several time slices where the time refers to the start of the high power phase. Increased peaking and expansion of the density profile is shown in Fig. 9(b).

A number of discharges were produced with both an internal transport barrier and a mild edge transport barrier associated with an ELMy H-mode. The pressure relaxation associated with ELMs were mild and did not affect the ITB greatly. In such cases, a maximum of 6.2 MW of fusion power was obtained. This is lower than the case shown in Fig. 8 but such discharges have a potential of being developed for steady-state high D-T fusion yields.

3.2.6 Fusion Power Development and Direct Extrapolation of JET D-T Data to ITER.

The fusion power development is shown in Fig. 10 where we show the 11% T in D experiments carried out in JET in 1991 and the best fusion power output (10.7 MW) discharge in the Supershot regime from the D-T campaign in TFTR from 1993-1997. Also shown are some of the best results obtained in JET in 1997 with a fusion power output of 16.1 MW obtained transiently in the hot-ion H-mode as well as the long-pulse steady-state fusion power output of 4 MW obtained in the ELMy H-mode regime. These results are promising and further D-T experiments are being considered to achieve improved fusion performance by operation at higher B_ϕ, improved current profile control and increased auxiliary heating powers. The scaling of energy confinement based on JET D-T and hydrogen data presented in section 4.3 concludes that large ELMy H-mode plasmas are dominated by gyro-Bohm transport. With this assumption, the energy confinement in ITER D-T plasmas can be predicted by using the JET data obtained in ~50:50 D:T plasmas directly. The experimentally obtained thermal energy confinement time in such plasmas is plotted in Fig. 11 using the gyro-Bohm transport scaling in dimensionless form with an isotope mass value of 2.5. This data is then compared with the ITER requirement for ignition at appropriate parameters in ITER simulations. We note that the JET data extends over more than one order of magnitude in normalized confinement time and that a similar gap exists between the top of the JET data and ITER. The extrapolated confinement time is in line with the

ITER expectation of 6s required for ignition. One of the main sources of uncertainty in this extrapolation lies in the high current data which does not have the β required for ITER due to a lack of input power in these shots.

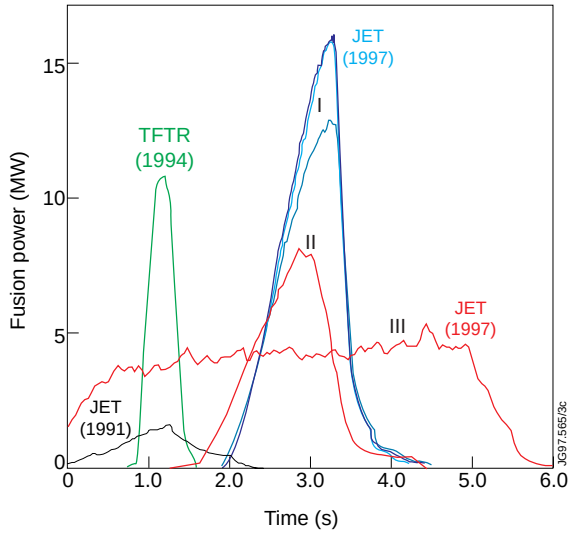

FIG. 10. Fusion power development in the D-T campaigns of JET and TFTR. (I) Hot ion H-modes, (II) Optimized shear and (III) Steady-state ELMy H-modes.

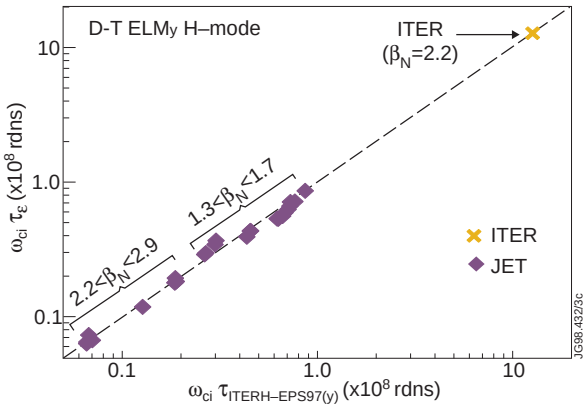

FIG. 11. Thermal energy confinement time data of JET D-T shots in dimensionless form is plotted as a function of the scaling obtained from the gyro-Bohm transport model. The ITER expected value of confinement in D-T plasmas is in line with that extrapolated from the JET D-T data.

This uncertainty can be removed in extrapolation to ITER based on specific steady-state JET D-T discharges [7] in which the toroidal β and the collisionality ν* achieved in JET is maintained in ITER. Dimensionless scaling constraints permit to extrapolate the stored energy for fixed β as

$$W_s \propto B^2 a^3 \qquad (4)$$

where B is the toroidal field and a is the plasma minor radius. Noting that the fusion power is proportional to the square of stored energy near the optimum ion temperature, we deduce scaled fusion power output in ITER corresponding to the JET discharges, knowing from ITER calculations that 1100 MJ of stored energy would produce a fusion power output of 1500 MW. Note that this result is based on ITER assumptions on impurity content, profiles and density which may not be identical to values achieved on JET. The input power needed to sustain the above stored energy is calculated based on gyro-Bohm and Bohm scaling of energy confinement time. The predicted Q values [7] are given in Table 3 for both the above gyro-Bohm and Bohm scalings. We note that ignition (Q=∞) can be achieved with relatively low β_N=1.7 and low $q_{\psi 95}$, though at a somewhat reduced power output of 1053 MW. Extrapolation based on this particular shot shows that reasonable value of Q~7 can be obtained even with the very pessimistic assumption of Bohm transport throughout the plasma.

Table 3: Extrapolation to ITER based on JET Steady-state D-T Discharges

Scenario	gyro-Bohm	Bohm
q_{95}=3.4, n =1.5n_{GW} I_p=21MA, β_N=2.4	Ignition 1.8 GW	Q=5.8
q_{95}=2.76, n =n_{GW} I_p=24MA, β_N=1.7	Ignition 1.05 GW	Q=7

4. ITER PHYSICS ISSUES

In this section, we discuss the results related to ITER physics issues. First, we present the results of α-particle heating and an experimental study of toroidal Alfven eigen (TAE) modes. We then discuss the scaling of H-mode power threshold, global energy confinement and turbulence followed by core and edge confinement physics issues. Subsequently, results of divertor operation and density limits and of tritium transport studies are presented. Finally we illustrate some of the ICRH results in D-T divertor plasmas.

4.1 Alpha-Particle Physics Issues.

Alpha particles (birth energy: 3.5 MeV) produced in D-T fusion reactions carry 20% of the fusion power. The success of a steady-state power-producing magnetic-confinement fusion reactor depends critically on harnessing this 20% of the power for continued plasma heating and sustaining the fusion reactions. A study of α-particle production, confinement and the resulting plasma heating, therefore, constitute an important physics issue for next-step devices such as ITER. Uncontrolled losses of α-particles can also damage the plasma facing components. These energetic particles, for example, can be lost by (i) first orbit losses, (ii) ripple trapped losses, (iii) stochastic toroidal-field ripple diffusion and (iv) collective effects relating to the α-particle interaction with MHD instabilities and RF waves such as toroidal Alfven eigenmodes and ion-cyclotron instabilities respectively. Plasma currents of more than 2.5 MA in JET and TFTR are sufficient to minimize the first orbit losses. In JET with 32 TF-coils, the ripple is very low so that ripple induced losses are insignificant. The α-driven collective effects such as TAEs and ion cyclotron emission depend critically on the α-particle pressure. In the present DTE1 campaign in JET, this pressure is expected to be close to the marginal stability. Therefore, α-particle heating experiments in JET are expected to provide a relevant test of the theory.

4.1.1 Alpha-particle Heating.

In the highest fusion performance D-T discharges in TFTR and JET, the α-particle heating is a relatively small fraction of the total heating power. However, heating with NBI only at a reduced power level, the contribution of the alpha particles to the electron input channel can be significant and clear T_e increases are expected when the D:T mixture is close to 50:50. Alpha particle heating has been revealed in this way by performing discharges differing only by the D:T concentration [12].

The above method has also been applied on JET: NBI heating at a level of 10 MW was applied where the plasma mixture was scanned from pure deuterium to pure tritium. The scan was performed using matched NB, gas fuelling and wall loading to avoid temporal or spatial variations in the D-T mixtures from shot-to-shot. The peak T_e obtained in each discharge of the scan is plotted in Fig. 12 as a function of the α-heating power deduced from the fusion power (neutrons) produced. It can be seen that the electron temperature rises linearly with fusion power and that the maximum T_e in JET data is observed at the expected D-T mixture of about 50:50 to 40:60. In pure D-plasmas, the T_e is the lowest. In T-rich mixture, T_e is also low and this rules out a possible isotopic effect on confinement. This is a clear demonstration of electron heating by α-particles in fusion power producing discharges. For comparison, we have also plotted two data points (D-T mixture of 100:0 and 50:50) of TFTR where α-particle heating was also apparent.

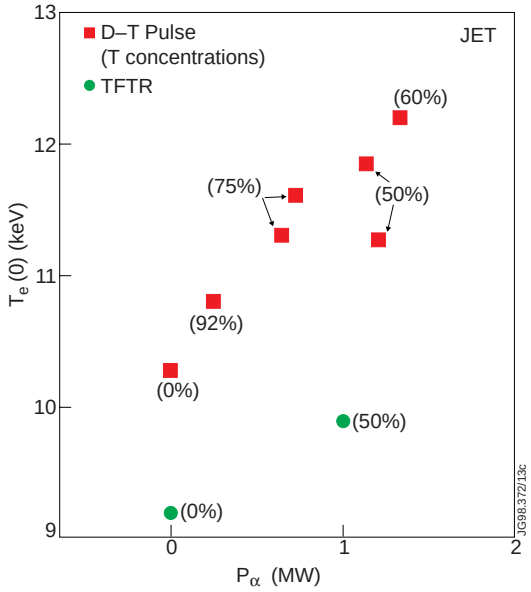

FIG. 12. Central electron temperature versus alpha-particle power in JET D-T discharges where the NBI input power was kept at about 10.5 MW . The numbers in parenthesis show the tritium concentration for this series of discharges. Also, shown are two data points of TFTR for comparison.

4.1.2 Toroidal Alfven Eigenmodes.

TAEs in tokamaks exist as discrete modes in the gaps of the shear Alfven continuum due to the effect of toroidal geometry. They can be driven unstable by energetic ions (such as α-particles, injected beam ions or those accelerated by ICRH) if the fast ion pressure is large enough to overcome the AE damping by the bulk plasma. The Alfven wave instability is predominantly associated with fast ion velocities (V_f) around or above the Alfven velocity ($V_A \equiv B_0/(4\pi\rho_i)^{1/2}$) where B_0 is the equilibrium magnetic field and ρ_i is the mass density of the bulk plasma ions. However, when toroidal precession of particles in a tokamak is taken into account, the modified wave-particle resonance conditions for circulating particles [51] lead to a range of resonant velocities, for example, from V_A to $V_A/3$. Resonant conditions for trapped particles are given in [51]. Previous experiments in D-plasmas have shown that TAE modes can be produced by energetic ions generated by NBI, for example, on TFTR [52] and DIII-D [53] and by ICRF heating on TFTR [54], JET [55,56] and JT60-U [57]. First potential observation of collective alpha particle effect on toroidal Alfven eigenmodes was made in D-T experiments on TFTR [58].

Several TAE modes with toroidal mode numbers ranging from n=5-11 have been observed on the magnetic fluctuation spectra in the high performance hot-ion H-mode discharges

heated by P_{NB}=18MW and P_{ICRH}=4.5 MW. These modes have been found [59] to be driven by ICRF-produced energetic ion tails and are shown in Fig. 13(a) where we plot the frequency of the modes as a function of time. In similar hot-ion discharges in D-T plasmas, but with lower $P_{ICRH} \leq 3.1$ MW, AE instabilities were not detected even when the central pressure of α-particles $\beta_\alpha(0) \approx 0.6$-0.7% was achieved at 16.1 MW of fusion power (see section 3.2.1). The absence of α-particle driven AE-activity is shown in Fig. 13 (b) where no magnetic fluctuations were seen in the expected frequency range in a discharge heated by NBI only. The fluctuations seen at lower frequency (<200 kHz) are usual low-level MHD activities that are normally present in such discharges. The absence of the α-particle driven AE-activity is in agreement with the CAS-TOR-K [60] stability calculations in this discharge as shown in Fig. 13 (c) where the instability regions due to α-particle driven AEs are shown as functions of α-particle average pressure ($<\beta_\alpha>$) and V_α/V_A (∝plasma density). The time evolution of $<\beta_\alpha>$ and V_α/V_A for the discharge shown in Fig 13 (b) is shown in Fig. 13 (c) and it is seen that the discharge remains in the stable region throughout [59]. The α-particle drive at the time of the peak performance for the fast growing mode (n=6) yields a normalised growth rate γ_α/ω =0.27% whereas the total damping rate is -1.41% out of which the bulk deuterium and tritium Landau dampings are -0.45% and -0.2% respectively, the high energy tritium beam damping is -0.53% and the sum of the radiative and electron collisional dampings is -0.23%. The large radial extent of the mode helps in its stabilisation. In some optimised shear JET D-T discharges, an AE instability is detected in the after-glow of the auxiliary heating. Similar observations have also been made in TFTR [14] where special effort was made to tailor the discharge so that AEs could be observed in the after-glow of the beam.

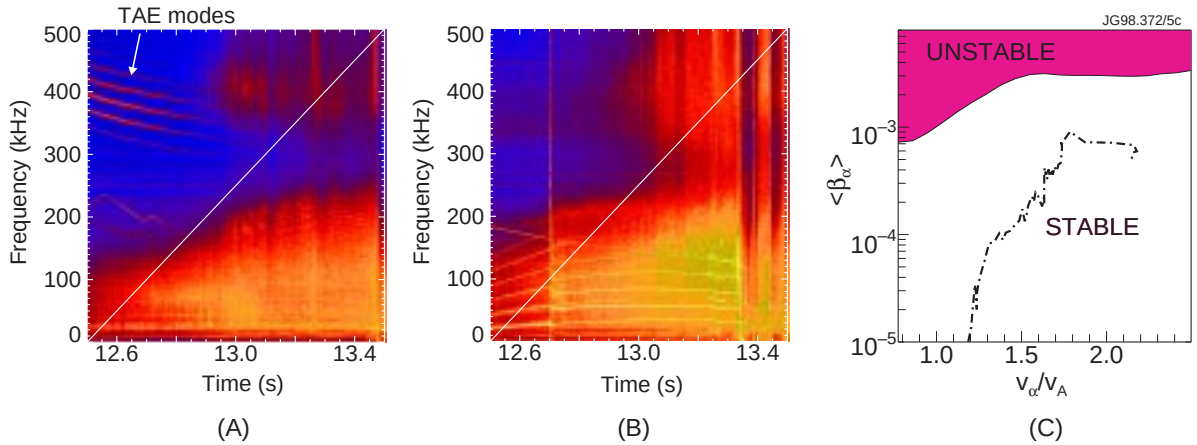

FIG. 13 (a). Spectrogram of the magnetic perturbations during an ELM-free period in a high performance deuterium discharge #40308 heated by 18MW of NBI and 4.5 MW of ICRH. Multiple AEs with different toroidal mode numbers ranging from n=6-11 are observed at the frequencies shown. (b) Same as in (a) but in a D-T discharge # 42677 heated by 22 MW of NBI only. In this case no AEs in the expected frequency range are observed. (c) The instability zone calculated by the CASTOR-K code for the alpha-driven AEs for the shot shown in (b). The time trace of the discharge in the $<\beta_\alpha>$ - V_α/V_A plane remains in the stable region in agreement with experiment.

4.2 H-Mode Threshold Power.

The realization of ITER performance relies on operating in the H-mode confinement regime to achieve ignition. Experimental data indicate that the H-mode operation requires that the power diffusing across the separatrix exceeds a threshold value. A scaling of the threshold power has been derived from the data from a number of tokamaks world-wide [61] but it has a scatter leading to a significant uncertainty (by a factor of 2-3) in the predicted value of H-mode threshold power for ITER. The above scaling gives explicit dependence on electron density (n_e), toroidal field (B_ϕ) and the tokamak major radius (R) but the threshold power is also found to depend on the direction of the ion ∇B drift, vessel wall conditioning, plasma-limiter distance, edge current density and on the isotopic mass. Here, we emphasize the isotope mass scaling of the threshold power for a more accurate assessment of the power required in ITER to access H-mode in D-T plasmas. In order to extend the mass range, experiments were also performed in hydrogen plasmas. Experiments were performed in quasi steady-state conditions in well conditioned walls with the ion ∇B drift pointing towards the X-point. The separatrix distance from the outboard limiters was > 5 cm.

Dedicated experiments have been carried out in JET with ICRH and NBI heating using slow ramps in power to determine the threshold power accurately. Plasma discharges with ITER shape and q at magnetic fields ranging between 1 and 3.8 T and densities in the range of 2 to 5 x 10^{19} m^{-3} have been used. For a set of parameters (B_φ =2.6T and I_p = 2.6 MA), in Fig. 14, we show time traces of $H\alpha$ /$D\alpha$ /$T\alpha$ and ICRH/NBI power in four shots with different gases: (i) H-plasma heated with H^0-NBI, (ii)-(iv) in three different D/T gas mixtures of 100:0, 50:50 and 10:90 respectively and heated with ICRH in H-minority scheme. As indicated in the figure, H-mode occurs (appearance of threshold or type III ELMs [62] in the $D\alpha$-signal) at the highest power in H-plasmas and at the lowest power in T-plasmas.

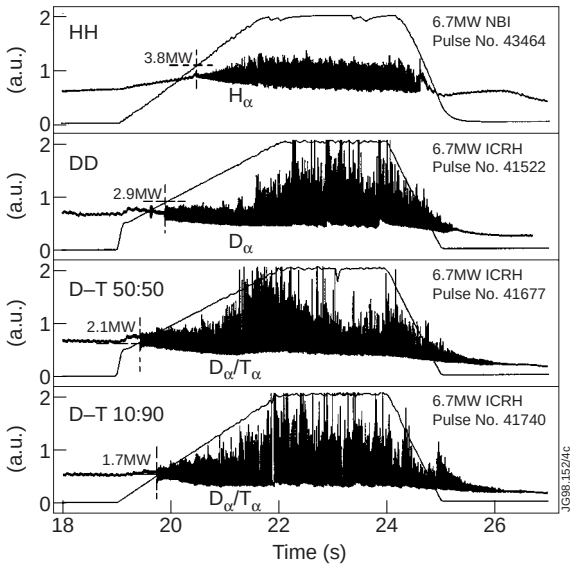

FIG. 14. $D\alpha$-signal and input power plotted as a function of time in four shots with different gas mixtures: hydrogen, deuterium, 50:50 D:T and 10:90 D:T. Same input power (6.7 MW) with a slow ramp was used to identify the onset of H-mode at the first appearance of ELMs as indicated. Threshold power decreases with increasing isotopic mass.

As the transition to H-mode is understood to be essentially an edge phenomenon, the power flowing outwards from the core and crossing the separatrix is chosen as the relevant parameter. Therefore, we define P_{SEP} to be the power crossing the separatrix:

$$P_{SEP} = P_{IN} - dW/dt - P_{RAD}^{bulk} \quad (1)$$

where P_{IN} is the total input power, W is the stored energy in plasma and P_{RAD}^{bulk} is the radiated power from the bulk of the plasma. A regression analysis has been carried out on the above defined loss power (P_{SEP}) at H-mode threshold for the JET data which includes a range of plasma current and magnetic fields in hydrogen and in D:T mixtures ranging form 100:0 to 10:90. In this analysis, in addition to using the same scaling parameters n_e, B_φ and R as in the scaling in [61], we have also included the isotopic mass (A) dependence. But, no regression was done on R as in the JET data, the value of R does not change significantly. The power exponent of R has been adjusted such that Eq. 1 below satisfies the constraint [63] to make the expression dimensionally correct. The result of this regression is shown in Fig. 15 and the power threshold scaling expression found is given by:

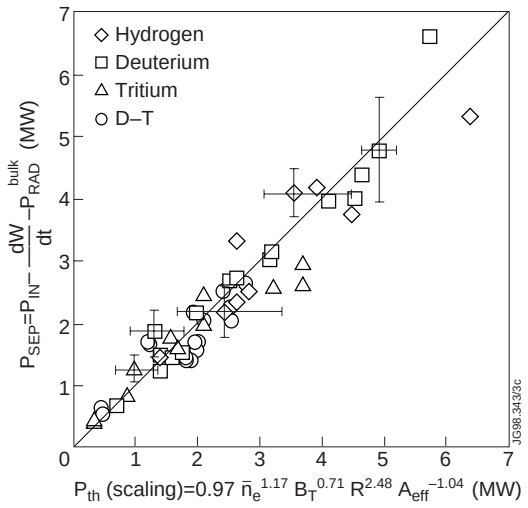

FIG. 15. The power crossing the separatrix (P_{SEP}) representing the L-H threshold power of JET discharges in hydrogen, deuterium, 50:50 D:T and 10:90 D:T mixtures is plotted against a scaling obtained by a regression analysis in which the A^{-1} mass dependence has been added to the ITER scaling [16]. This regression of JET data indicates an approximate inverse mass dependence of the threshold power. No regression has been done on R. Here, W is the plasma stored energy and P_{RAD}^{bulk} is the radiated power from the plasma bulk. The density n_e is in units of ($x10^{20}$ m^{-3}).

$$P_{th\,(SEP)} = 0.97\, n_e^{1.17}\, B_\varphi^{0.71}\, R^{2.48}\, A^{-1.04} \qquad (2)$$

Here, $P_{th\,(SEP)}$ represents the threshold power for a transition from L to a dithering H mode, n_e is the line-averaged electron density (in 10^{20} m^{-3}). The threshold power data shows roughly an inverse mass dependence. This predicts a significant reduction in the power needed for accessing the H-mode in D-T plasmas in ITER and increases the operational flexibility of ITER. For example in ITER, for n_e=5x10^{19} m^{-3}, B_φ=5.68T and R=8.14 m, the power required for L-H transition in a 50:50 D:T plasma is estimated to be P_{SEPth}=63 MW [15] which is 20% less than that needed in D-plasma.

It is expected that in a burning plasma in ITER, the power crossing the separatrix will be 30 to 50% above the H-mode threshold. At such a level, in a JET discharge with RF heating (see Fig. 7), the amplitude of ELMs is small and the ITERH97 confinement factor (~0.9) is adequate for ignition. Note, however, the plasma β in this discharge is significantly smaller than in ITER. Crash of such small ELMs have little or no adverse impact on the divertor target.

4.3 Global Energy Confinement and Turbulence

4.3.1. Global Energy Confinement.

With a view to predicting the energy confinement time in burning plasmas more accurately, JET has carried out dedicated experiments, the so-called ρ*-scaling experiments, in which carefully

constructed ITER similarity pulses are used to assess ITER relevant ELMy H-mode energy confinement [54]. Key physics dimensionless parameters such as β, ν^* and q are fixed at their ITER value save the dimensionless Larmor radius $\rho^*(\equiv\rho/a)$ The JET machine is the one closest to ITER with the smallest ρ^*-values within a factor of 5 from that of ITER. This parameter is varied in JET to determine the ρ^*-scaling of confinement and then extrapolated to ITER. After validation, the data will be included in the world confinement database which will benefit from the full range of ρ^* [48]. Here, with the availability of JET data in D-T plasmas, we emphasize the effect of the isotopic mass on the energy confinement scaling.

The isotopic mass scaling of the thermal energy confinement has previously been studied on ASDEX [64], DIII-D [65], JT60-U [66] and JET [67] using hydrogen and deuterium discharges. More recently, TFTR extended the mass scaling in the D-T experiments in a variety of modes of operation [4]. The mass dependence of the energy confinement time $\tau_{th} \propto A^{\alpha}$ varies in a wide range (α=0-0.85) depending upon the mode of operation. Theoretically, the gyro-Bohm turbulence model implies α=-0.2 and for long wavelength turbulence of the Bohm form, α=0 is expected.

The JET ELM-free H-mode confinement data in D-T plasmas is found to have a $A^{-0.25}$ mass dependence [70]. A comparison of this data with ITERH93-P scaling [68] concludes that its $A^{0.4}$ dependence is clearly too strong and does not fit the JET D-T data. However, the experimental $A^{-0.25}$ mass dependence is not far from fitting the $A^{-0.2}$ dependence of the gyro-Bohm physics form [69].

We now present the result of a comparison of the ELMy H-mode data which includes H, D, and D-T discharges heated by NBI and ICRH with the ITERH-EPS97y ELMy H-mode scaling. This scaling derived from an updated database has a weak mass dependence ($A^{0.2}$) and fits with the JET data reasonably well as shown in Fig. 16. Refitting the data by using the same form as ITERH-EPS97y scaling but allowing the mass and the constant in front to be varied, results in a better fit with a slightly weaker mass dependence of $A^{0.16}$ [18]. Due to the influence of isotope mass on H-mode threshold power and ELM behaviour, it is not always possible to obtain the same density for the same input power in all conditions of operation. If we constrain the data such that power (within 5%) and density (within 25%) in H, D, D-T and T-plasmas are matched, a regression analysis on this data presented in [7] shows that, in fact, the mass dependence is close to zero ($\sim A^{+0.03 \pm 0.08}$). A likely reason for the lower

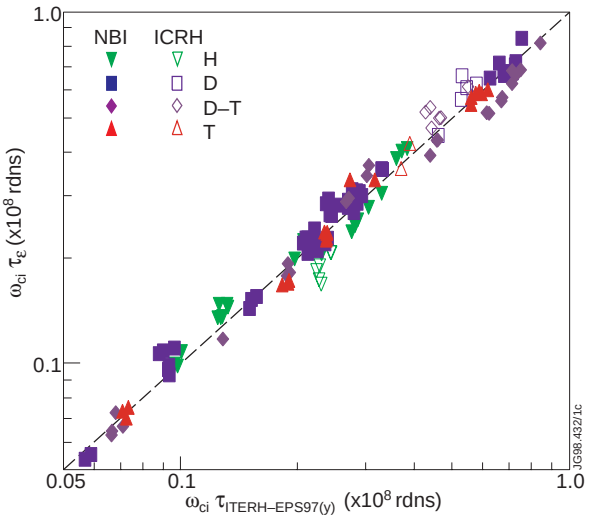

FIG. 16. Thermal energy confinement time is plotted as a function of the normalised ITERH-EPS97y scaling for the JET discharges in D-D, D-T and T-T plasmas heated by ICRH and NBI as indicated.

value of the exponent of A is due to the collinearity between the density and the A dependence. The operating density for the same input power is progressively lower in deuterium and hydrogen plasmas as compared to that in tritium due to higher frequency of ELMs as A increases [19].

To investigate the origin of the weak mass dependence in the global energy confinement time, we study separately the scaling of the calculated stored energy in the pedestal and that of the rest of the profile which we term as the 'core' plasma. The energy in the core (W_{core}) is obtained by subtracting the energy of the pedestal (W_{ped}) from the total stored energy. The pedestal energy (time averaged on steady-state ELMy H-modes) is plotted in Fig. 17 (a) as a function of $\sim I_p^2$ $((0.5A\ T_{pedth})^{0.5}/I_p) \sim I_p^2 = \rho_{i\ th}$ (see also section 4.4) for H, D and D-T and T-discharges. Symbols are defined in the figure caption. The scaling in Fig. 17 (a) shows a mass dependence of $\sim A^{0.5 \pm 0.2}$. However, as shown in Fig. 17 (b), the core energy confinement time has an $\sim A^{-0.17 \pm 0.1}$ dependence, very similar to that expected from the gyro-Bohm transport ($\sim A^{-0.2}$) model. Note that the observed scaling of the pedestal energy is consistent with a model in which the edge pressure gradient saturates at the ballooning limit over a region of width that scales as the ion poloidal Larmor radius (see below). Thus the net effect of the isotopic mass is negligible in the global energy confinement time [18] as the two effects roughly cancel each other. Since the ratio of plasma volume to its surface varies as R, one expects that the global energy confinement scaling becomes increasingly gyro-Bohm in larger tokamaks.

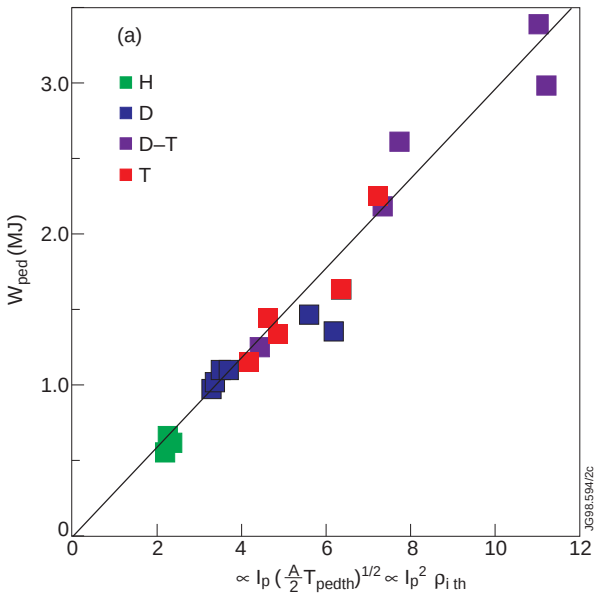

FIG. 17 (a). Pedestal stored energy (W_{ped}) in JET H-mode discharges is plotted as a function of $\sim I_p^2$ $(0.5A\ T_{pedth})^{0.5}/I_p) \sim I_p^2 \rho_{ith}$ for different isotopic mixtures of H, D and T. Here, I_p is the plasma current, A is isotopic mass, T_{pedth} is the measured electron pedestal temperature and ρ_{ith} is the ion Larmor radius assuming that the ion temperature is the same as T_{pedth}. Also, $W_{ped} = p_{ped} V$ where p_{ped} is the pressure at the edge pedestal and assumes equal electron and ion contributions, and V is the plasma volume.

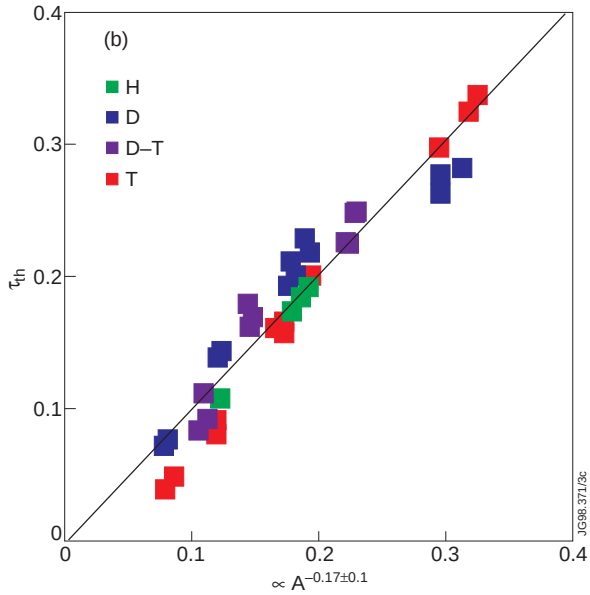

FIG. 17 (b). Core plasma thermal energy confinement time in H-mode discharges is plotted as a function of the gyro-Bohm scaling for JET discharges in different isotopic mixtures of H, D and T.

4.3.2. Turbulence.

Understanding the underlying physics behind the empirical scaling laws of tokamak confinement is important for building confidence in predictions and extrapolation to ITER. As mentioned before, there is a growing evidence that different physics is involved in different regions of the discharge. A leading candidate for ion thermal transport in the core region is the ion temperature gradient (ITG) driven turbulence. In the ITG model, the ion transport scales like gyro-Bohm ($\chi \sim \rho^* T/B$) where ρ^* is the normalized (by tokamak minor radius) ion Larmor radius. Several experiments (DIII-D and TFTR) have shown that the core turbulence in the H-mode phase is intermittent or burst-like in nature. While we have not been able to identify the cause of anamolous transport in JET, nevertheless, intermittent turbulence (or increased density fluctuations) has been seen [71] in many types of JET discharges such as hot-ion ELM-free and ELMy H-modes and optimized shear discharges. An illustration of bursts of density fluctuations is shown in Fig. 18 where intensity contours of log spectral intensity are plotted in a frequency-time plane. The data shown pertains to a 2T/2MA steady-state ELMy H-mode 14:86 D:T discharge heated by 10.5 MW of NBI. These measurements of phase fluctuations (correlated with density fluctuations) are made by microwave X-mode reflectometer at about R=2.55m determined by the cut-off density. These bursts in fluctuations appear periodically but their frequency does not appear to be constant. In the time window shown, the frequency varies from from 120 kHz to 10kHz. The level of background turbulence is also seen to rise and fall. The product of the burst duration and its amplitude are found to be roughly constant.

The origin of intermittency in the plasma turbulence can be intuitively expected from the following mechanisms [72]. In the ITG model, the growth rate of the instability rises strongly above a certain threshold in the ion temperature gradient and the maximum growth rate $\gamma_{max} \sim k_\perp \rho_i \sim 1$. As the fluctuation level increases, the dT_i/dr decreases and spectral density is shifted towards low-k (long wavelength) values. This, in turn, drives an electric field which produces a $v_\theta = \mathbf{E}x\mathbf{B}/B^2$ drift velocity, the gradient of which produces a stabilizing effect on the instability and the turbulence would be suppressed. When the dv_θ/dr stabilization exceeds the instability growth rate γ_{max}, the dT_i/dr rises and the turbulence starts again. This alternation of self-stabilization and destabilization produces the effect of intermittance in turbulence. The repetition rate depends upon γ_{max}.

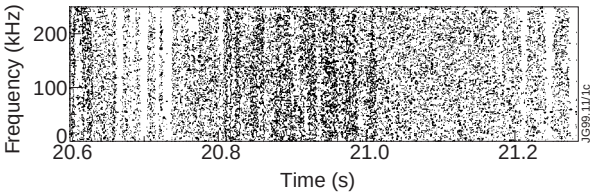

FIG. 18. A contour plot of spectral intensity of the reflectometer phase fluctuations at R~2.55 m (r/a~0.5) in the frequency-time plane for the JET shot #42808. Note that the intermittent bursts of fluctuations observed in this shot are not correlated either with ELMs, sawteeth or rotating MHD modes.

4.4 Edge Localised Modes and Pedestal Width.

Edge localised modes (ELMs) are MHD-like instabilities which occur during H-modes and produce bursts of energy and particles that are ejected through the separatrix to the scrape-off layer and ultimately end up predominantly in the divertor. We have studied the behaviour of ELMy H-mode discharges heated by NBI and ICRH in terms of edge pressure gradient in H, D, and D-T plasmas [19]. Assuming that the critical edge electron pressure ∇p_e^{crit}, just before the crash of an ELM is limited by the ballooning instability, we obtain the scaling expression: $\nabla p_e^{crit} \propto I_p^2 s$ [19] where I_p is the plasma current and s is the magnetic shear at the edge. Approximating ∇p_e^{crit} by p_e^{crit} / Δ, we can write

$$p_e^{crit} \propto I_p^2 s \Delta \propto I_p s (AE)^{1/2} \quad (3)$$

where E is the averaged energy of the ions in the edge and Δ is the width of the edge transport barrier which is assumed to be governed by the ion Larmor radius ρ_i. Edge electron pressures for a series of shots heated by NBI and ICRH show the NBI experimental data increases somewhat more strongly than $A^{1/2}$ whereas the electron pressure for the ICRH data is much smaller and is practically independent of the isotopic mass [19]. Thus the scaling derived from Eq. 3 does not represent adequately the observations.

An analysis presented in Ref. 17, discusses the correlation of the transport barrier width Δ with the edge ion thermal energy or with the energy of the fast-ions residing in the edge. This scaling represented by Eq. 3 is further evaluated for a number of JET (non additionally fuelled) discharges in which the safety factor q is held constant but B_ϕ and I_p are varied in a range of 1.7-2.9 T and 1.7-2.9 MA respectively. Also, the value of magnetic shear s at the edge is varied between 2.9 to 4. The peak edge pressure just before the occurrence of ELMs is then compared against the pressure estimated theoretically at the ballooning limit using the simplified formulation discussed above. For illustration, we show the two fits for comparison, one with ρ_{Lfast} and the other with $\rho_{Lthermal}$ in Figs. 19 (a) and 19 (b) respectively. It is seen that the scaling of the peak edge pressure based on the ion poloidal Larmor radius determined by the fast-ions in the edge (ρ_{Lfast}) gives the better fit. However, the pedestal energy (W_{ped}) time averaged over steady state discharges [18] is better correlated with ρ_{ith}. Note that these two (peak and average) edge quantities are different and need not scale in the same way although, in both cases, the strong mass scaling ~$A^{0.5}$ is the same. Dedicated experiments are planned to identify more directly the role of fast ions on edge stability.

A comparison of ELMs with ICRH and NBI has been done previously [73]. It is found that ELMs produced by ICRH have higher frequency and lower amplitude. At a given power input, the repetition rate and amplitude of ELMs is relatively less steady as compared to NBI but the energy confinement is about the same in the two cases. It is also found that power deposited on divertor tiles per ELM is smaller by a factor 2-5 as compared to beams. In both NBI and ICRH cases, the ELM frequency decreases with isotope mass and as mentioned above the ELM frequency is higher in the ICRH case by a factor of about 10-12 [19].

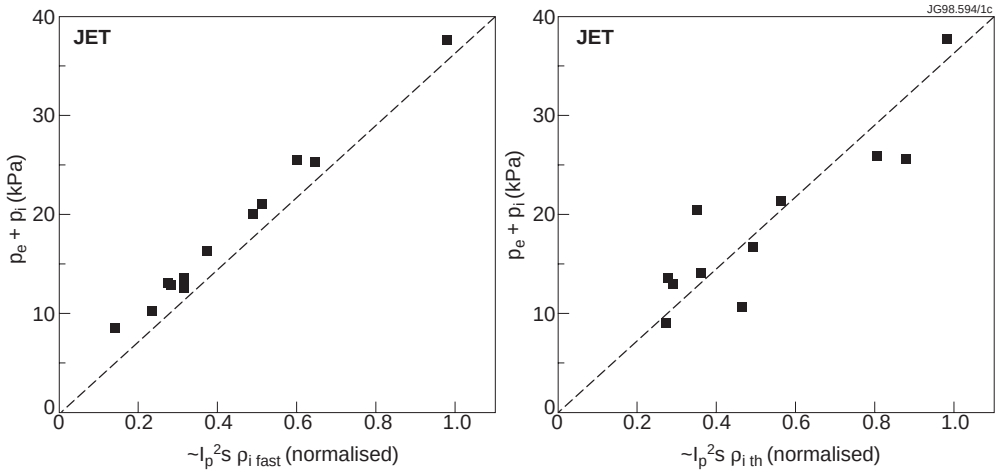

FIG. 19 (a). Experimental data of total (electron and ion) edge pedestal pressure (symbols) is plotted against the normalized expression ($I_p s (A<E>_{fast})^{1/2}$) based on the fast-ion averaged energy in the edge. The data represents the peak edge pressure before the ELMs. (b). Experimental data of total (electron and ion) edge pedestal pressure (symbols) is plotted against the normalized expression ($I_p s (A<E>_{thermal})^{1/2}$) based on the thermal ion temperature in the edge. See the caption of Fig. 11.

4.5 Divertor Operation and Density Limits

The density limit in tokamaks fueled with gas puffing and auxiliary heating is often represented by the empirical Greenwald limit [74] $n_{GW}\,(10^{20}m^{-3}) = I_p(MA)/\pi a^2(m^2)$. For achieving its rated maximum fusion power (1.5 GW), ITER has to be operated at 10-20% higher density than n_{GW} in ignited regimes or at ~ n_{GW} in the driven mode. Thus it is important to understand the underlying physics of density limits in tokamaks and find ways to increase the central density without degrading the confinement.

A routine observation in JET is that at a given input power, increasing the plasma density in ELMy H-modes by increased gas fuelling leads to a degradation in global particle confinement. At some point, this loss outweighs the additional gas fuelled particle source and an effective density saturation is reached [20] without undergoing a disruption. As the density limit is approached, the thermal energy ELMy H-mode confinement time also degrades as compared to the ITERH97y value. This is illustrated in Fig. 20, where we provide data on a comparison of deuterium and tritium gas puffed discharges heated with 11-12 MW of NBI power at 2.6T/2.6MA. We note that the ELMy H-mode thermal energy confinement time both in deuterium and tritium plasmas decreases significantly when the plasma density exceeds 0.75 of the Greenwald (n_{GW}) limit.

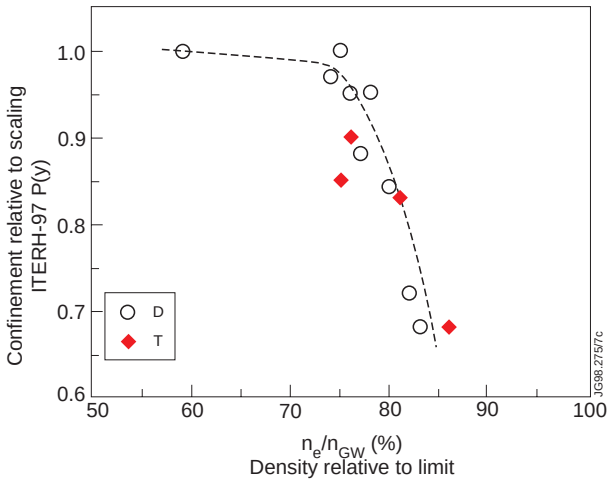

FIG. 20. Thermal energy confinement time normalized to ITERH-93Py scaling is plotted against plasma density normalized to Greenwald density limit (n_{GW}) [74] in JET discharges made in 100:0 and 10:90 D:T gas mixtures.

Both in deuterium and tritium discharges, the maximum density achieved is $0.85n_{GW}$. Note that the degradation in energy confinement with additional gas fuelling is related to the lowering of the pressure pedestal. At low and moderate gas rates, the confinement degradation is predominantly at the edge. At higher rates, the region of confinement degradation starts to expand from the edge to the core [20].

4.6 Trace Tritium Particle Transport.

A knowledge of particle transport properties of a confined plasma is required for the reactor fueling requirements as well as for the plasma density control and the control of fusion power. To determine the tritium transport properties, the neutron profile monitor has been absolutely calibrated to provide line integral neutron yield. A 1 _ -D transport model [75,76] with diffusive and convective terms as well as a dynamic recycling model which describes the response of the wall to changes in the isotopic composition is used. The beam-thermal and thermal-thermal reactivities are also modeled. A least-square fit of parameters of the model to chordal neutron data together with a knowledge of the error bars on the signal permits the derivation of the transport coefficients.

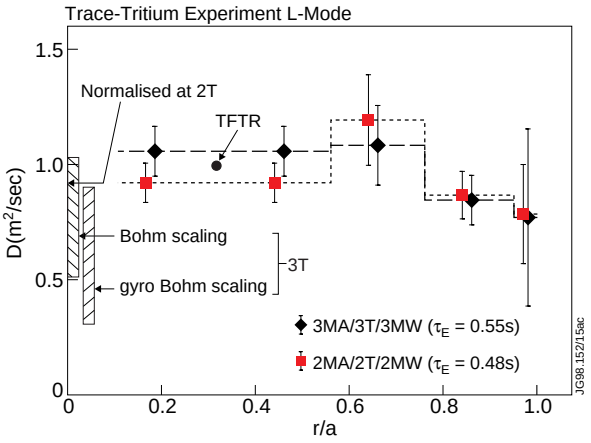

FIG. 21 (a). Profile of particle diffusivity (D) derived from JET trace tritium ITER similarity L-mode plasmas in deuterium at 2T/2MA and 3T/3MA. Normalised to 2T data, the expected band of values at the centre for Bohm and gyro-Bohm scalings for 3T are also shown schematically. The shaded bands represent the uncertainty in central T_i measurements.

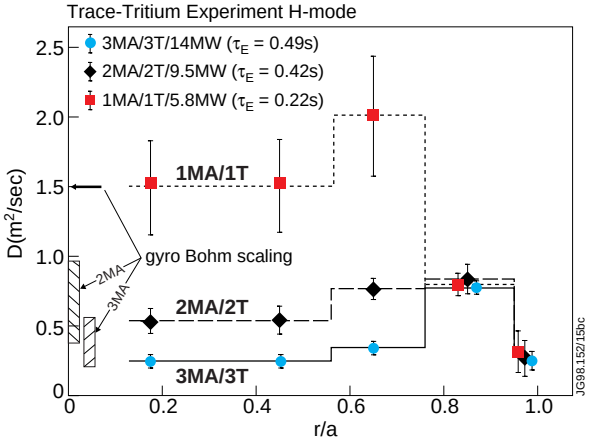

FIG. 21 (b). Profile of particle diffusivity (D) derived from JET trace tritium ITER similarity H-mode plasmas in deuterium at 1T/1MA, 2T/2MA and 3T/3MA. Normalized to 1T, the expected band of values at the centre for gyro-Bohm scaling for 2 and 3T are also shown schematically. The shaded bands represent the uncertainty in central T_i measurements.

Profiles of tritium diffusion coefficient (D) in L-mode and H-mode discharges have been inferred using the above procedure (see Fig. 21). Tritium was puffed in these deuterium discharges which were similar to the ρ*-scaling discharges discussed above having ITER shape, q, β and ν*. The discharges used in L-mode were at B_ϕ/I_P of 2T/2MA and 3T/3MA heated with 2 and 3MW of NBI power respectively whereas in H-mode, 1T/1MA, 2T/2MA and 3T/3MA discharges heated by 5.8, 9.5 and 14 MW of NBI power respectively were used. Bohm and gyro-

Bohm scalings of D are proportional to T_i/B_ϕ and $T_i^{3/2}/B_\phi^2$ respectively where T_i is the ion temperature. The measured values of D in L-mode discharges is close to 1 m^2/s both for 2 and 3T discharges. Normalizing to the 2T discharge, the expected band of values of D of the 3T discharge based on Bohm and gyro-Bohm scalings are shown in Fig. 21 (a). The uncertainty in T_i measurements is reflected in the shaded areas shown. The data in L-mode is slightly closer to the Bohm value, but the uncertainties in the measurement of T_i and D do not allow us to rule out one or the other. However, in H-mode discharges, the observed strong variation of D with B_ϕ for r/a<0.75 indicates a marked gyro-Bohm character in the core region. In this case, normalizing to the 1T discharge, the expected band of values of D of the 2 and 3T discharges are as shown in Fig. 21 (b). For the edge region ($0.75 < r/a < 0.95$), D does not depend on B_ϕ, and points to Bohm scaling but again with a large uncertainty. Thus we note that in H-mode, both the energy and particle diffusivities have a gyro-Bohm character in the core whereas in the edge-region, no definite conclusions can be reached due to large uncertainties in the measurements.

4.7 ICRH Experiments in D-T Plasmas

Second harmonic heating of tritium ($2\omega_{CT}$) and deuterium minority heating at fundamental cyclotron frequency (ω_{CD}) are the two Fast-wave reference heating scenarios for ITER. TFTR has already observed efficient heating in ICRH D-T experiments performed at $2\omega_{CT}$ in circular limiter plasmas using a $(0,\pi)$-phased 2-strap antenna [21]. JET has repeated similar experiments extending the operational domain to D-minority heating (ω_{CD}) and to ITER-like configuration [22] with $0\pi0\pi$-phasing of the 4-strap ICRH antennae similar to the reference ITER antenna design. Results of D-minority heating in tritium with the achievement of steady-state $Q\approx0.22$ with ICRH alone have already been presented in Section 3.2.4. Strong single-pass damping (more than 90%) experiments in JET with hydrogen minority in tritium [77] plasmas are akin to those that will prevail in ITER.

Second harmonic heating of tritium ($2\omega_{CT}$) experiments were carried out using freshly reprocessed tritium to minimize the content of He^3 in the plasma due to radio-active decay of tritium so that He3 minority ion absorption is avoided. Experiments in this scheme have been carried out at a level of 8 MW of ICRH power. Since the damping rate in this scheme increases with the resonant ion energy, large triton energy tails can be produced for bulk ion heating. Despite operating at high plasma density ($5x10^{19}m^{-3}$) the tail energy was still in the electron drag regime. This regime will change to ion heating in ITER where the power density is much reduced. Calculations with PION code show that 70% ion heating fraction can be achieved along the route to ignition with 50 MW of ICRH power. The power density is kept close to $300kW/m^3$ by using two resonance layers to broaden the power deposition.

Puffing a small amount (>2%) of He^3 (in addition to the He^3 present due to radio-active decay) improves significantly the energy confinement [78]. In such a case, minority (He^3) ion

absorption dominates (as in (H)-D plasma), single pass absorption increases and a significant He^3 tail is produced. By adding He^3 to a level of 5-10 %, the He^3-tail energy is lowered below the critical energy to produce strong ion heating. Time traces of such a discharge are shown in Fig. 22 where $T_{i0}\approx 13$ keV is achieved by ICRH alone. He^3-minority heats ions more efficiently than tritons resonating at $2\omega_{CT}$ as the averaged energy of the He^3-tail is smaller. Central electron and ion temperatures in this discharge are roughly equal. Also, the ITERH97 factor is higher, nearly unity in this case . These results of heating at $2\omega_{CT}$ and those of He3 minority heating are well simulated by PION code and give confidence in its prediction for ITER. The experimental results including the strong bulk ion heating obtained at JET and TFTR constitute a firm experimental basis for the application of ICRH on ITER. Bulk ion heating predicted by PION for ITER provides more alpha particle heating for a given additional heating power input and can be an advantage for easier access to the H-mode and for higher Q in driven modes.

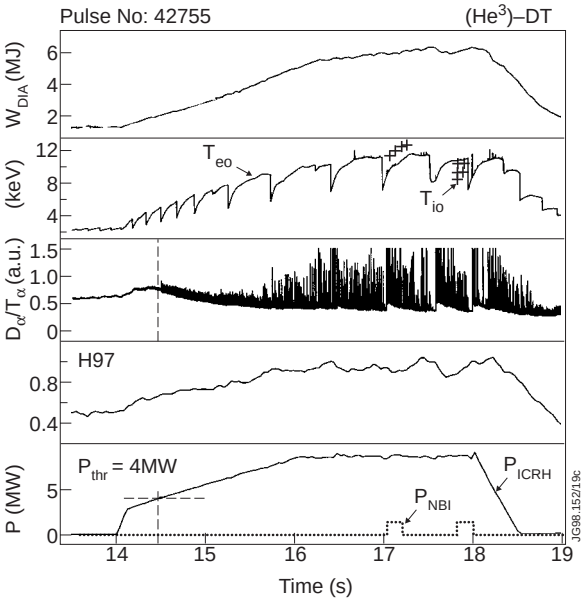

FIG. 22. Time traces of a He3-minority ICRF heating of a 45:55 D:T plasma with about 10% of He3 added. Other parameters are B_φ=3.7T, I_P=3.3MA, f=37.2MHz, and $n_{e0}=3.2\times10^{19}m^{-3}$. Central electron and ion temperatures are 12 and 13 keV respectively. The ITERH97-Py factor is close to unity.

5. FUSION TECHNOLOGY

The technological goal of the JET DTE1 experiments was to demonstrate key reactor relevant technologies: tritium handling, processing and mixture control, remote maintenance and installation. Moreover, it was necessary to demonstrate that these operations can be carried out safely without significant discharges of tritium to the atmosphere and limit the radioactive exposure to site personnel to well below the prescribed limits.

5.1 Tritium Processing.

With its Active Gas Handling System (AGHS), JET has tested the first large scale plant [24]for the supply and processing of tritium in a closed cycle which includes an operating tokamak. This plant collects gas from the torus, removes impurities from hydrogen, isotopically separates the hydrogen gas into streams of protium, deuterium and tritium. This plant stores the deuterium and tritium in U-beds for re-use and injects them back to the torus when desired. The isotope separation makes use of cryo-distillation and gas chromatography. This plant supplied 100g of

tritium to the NBI boxes and the torus allowing the repeated use of the 20g of tritium brought on-site. The AGHS operated reliably throughout the DTE1. The total atmospheric discharge of tritium during DTE1 was less than 2 TBq which compares very well to JET's authorization for safe discharges of tritium as oxide of 20 TBq/month and 90 TBq/year.

5.2 Remote Handling.

The JET 1998 programme includes the experimental assessment of a new gas box divertor (MkIIGB). Activation inside the torus resulting from the tritium phase excludes the possibility of man intervention for about 18 months after DTE1. A replacement of the divertor target structure by full remote handling techniques [25] was therefore planned. The establishment of the procedures as well as the training of the operators was rehearsed in the In-Vessel Training Facility. The remote tile exchange was carried out successfully in about 4 months which removed all 144 MkIIA divertor modules and replaced them with 192 MkII Gas-box Divertor modules. Maintenance of a number of in-vessel protection tiles was carried out and some of the diagnostics systems were also removed and installed remotely. A photograph of the in-vessel components and the Gas-box divertor configuration is shown in Fig. 23 together with the remote handling manipulation.

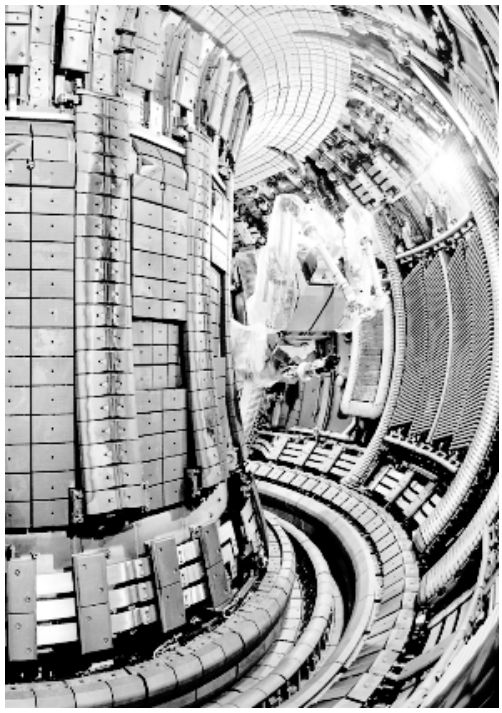

FIG. 23. A photograph of the inside view of the JET tokamak showing the MkII Gas-box divertor on the floor. The divertor tiles were installed by the remote handling tool shown above. Also shown are the ICRH antennae and the LHCD launcher on the right-hand side of the picture.

6. DISCUSSION AND CONCLUSIONS

We have presented, in this paper, a review of JET experimental results and the underlying physics of JET and TFTR D-T tokamak plasmas. In these experiments, the D:T mixture was varied from 0:100 to 10:95. Operation in tritium rich mixture allowed new regimes to be exploited. A number of modes of operation have been developed in the TFTR (circular, limiter) and JET (non-circular divertor) tokamaks. The maximum fusion power output of 16.1 MW was achieved in JET in the hot-ion H-mode plasmas heated by NBI (22.3 MW) and ICRH (3.1MW) with a fusion amplification factor $Q \approx 0.62$. A steady-state discharge produced a fusion power of 4 MW and a $Q=0.18$ for 3.5 s. A clear demonstration of α-particle heating has been made. The need for good D-T mixture control for high fusion performance was clearly demonstrated. With a view to

reactor physics issues, emphasis was placed on the study of the dependence of isotope mass on important quantities such as H-mode threshold power, energy confinement, ELMs, edge pedestal and density limits in tokamak plasmas. To extend the mass range, results of dedicated experiments carried out in hydrogen after the DTE1 campaign have also been presented. Experiments were carried out in plasmas with plasma geometry and q similar to ITER and special efforts were made to match the key physics dimensionless parameters such as β and ν^* to their ITER value. The main scaling parameter ρ^* was varied to determine the related confinement scaling and then extrapolate to ITER. The electron and ion temperatures were very close to each other as expected in a reactor. Results of experiments conducted to validate the ICRH reference scenarios in reactor have also been presented.

These results have the following important implications for fusion reactor development:

(i) From experiments in H, D and T-plasmas, a clear reduction in H-mode threshold power is seen as the isotope mass is increased. A regression analysis of JET data is consistent with an inverse mass dependence of threshold power. This result has a favourable consequence of reducing by about 20% the power requirement in ITER (in 50:50 D:T as compared to the D-D operation) to reach the high confinement regime and widens the ITER route to ignition. Note also, that the above results of power threshold are independent of heating method.

(ii) JET results show that the global energy confinement is practically independent of isotopic mass. The confinement in H-mode plasmas is considered to be composed of two parts: (a) the core which is governed by the physics form of gyro-Bohm transport ($\sim A^{-0.2}$) and (b) the ELMy edge in which the pedestal energy scales as $\sim A^{0.5\pm 0.2}$. This leads to the result that the net effect of isotope mass on global energy confinement is negligible for the JET size device. This difference in mass scaling of the core and the edge emphasizes the importance of JET which is less dominated by plasma edge effects than smaller machines. In the final analysis, the unfavorable mass dependence, as compared to the earlier ITER projections, is compensated by the stronger density dependence found in the JET data. This is confirmed in Fig. 11 where the ITER confinement time required for ignition is in line with the JET D-T data albeit following different power coefficients of density and isotope mass than the earlier scaling. Note that this extrapolation assumes that the reactor could be operated near the Greenwald density limit without a significant degradation of confinement in contrast to what JET finds using gas fuelling.

(iii) High current, high power near steady-state discharges with q and plasma geometry similar to ITER in 50:50 D:T plasmas achieved high performance with fusion power output of 4 MW and a $Q \approx 0.18$ in which type I ELMs are maintained throughout the discharge for more than 3.5 s. This lends strong support to the reactor mode of steady-state operation with type I ELMs assuming that the problem of target erosion during type I ELMs can be resolved satisfactorily by appropriate divertor design. Discharges heated with ICRF alone

in D-minority scheme produce a steady-state Q≈0.22 at an input power of 6MW where the neutrons were of non-thermal origin. Note that with ICRH both small ELMs and good confinement could be maintained simultaneously.

(iv) An extrapolation of the performance of steady-state JET D-T discharges to ITER has been made based on stored energy achieved and assuming gyro-Bohm or Bohm scaling of the energy confinement. Using the former scaling, ignition (Q=∞) in ITER with a fusion power output of 1.05 GW is predicted based on the JET steady-state discharge featuring a β_N =1.7 only. For the same discharge, a Q=7 can be achieved when the pessimistic Bohm scaling is used.

(v) The observed scaling of the edge pedestal energy ($\sim A^{0.5\pm 0.2}$) is consistent with a model in which the edge pressure gradient saturates at the ballooning limit over a region of width that scales with the ion poloidal Larmor radius. Present results suggest that edge fast ions could play an important role in the edge stability. Further experiments are planned to clarify this important aspect for a reactor.

(vi) The tritium transport experiments in H-mode indicate that for r/a < 0.75, the particle diffusivity exhibit gyro-Bohm scaling whereas for 0.75 < r/a < 0.95, it points to the Bohm scaling with a large uncertainty.

(vii) ICRH reference scenarios for a reactor (tritium second harmonic and deuterium-minority heating) in D-T plasmas have been successfully tested. A small concentration of He3 added in the former scheme produced strong bulk ion heating ($T_{i0} \approx 13$ keV) due to improved power localization and lower He3 tail energies. A good agreement is found between PION code predictions and experimental results. The present ICRH results obtained on JET constitute a firm experimental basis for the application of ICRH in a reactor. In particular, the significant bulk ion heating will facilitate an easier access to the H-mode regime and could also provide higher Q in the driven mode of a reactor.

The combination of JET features such as large-scale plasma, flexible heating and current-drive systems, ITER-like divertor configuration with C and Be for plasma-facing components and operation in D-T plasmas have made JET a unique device for making essential contributions to the reactor modes of operation. Overall, the JET results obtained in D-T plasmas are a welcome news for a reactor. Moreover, the on-site closed-cycle tritium reprocessing plant and remote handling tools at JET have provided an integrated demonstration of a safe and reliable operation in reactor-relevant conditions.

Nevertheless, significant work remains to be done to consolidate the physics of burning plasmas which will guide the future programme of JET. The two high-fusion performance (hot-ion H-mode and optimised shear) regimes can be further developed to increase the fusion power production with a view to improving the demonstration of α-particle heating. However, these presently transient regimes, need also to be developed for long pulse operation. This could be achieved with measures for controlling the steep gradients in the edge transport barrier. The

optimised shear scheme is the best candidate for steady-state reactor operation. The internal transport barrier and its coexistence with an ELMy edge is likely to require active real-time profile control. The other most important future work for the burning plasma operation includes:

(a) A confinement database to be constructed near operating boundaries with data at or near the Greenwald density limit, at lower q (~2.7) and at the ITER values of β_N. This will require systematic use of deep fuelling methods and a substantial increase of the additional heating power.

(b) A clear understanding of the physics of accessing the H-mode and, in particular, reducing the uncertainties in the power exponents of plasma parameters appearing in the H-mode threshold scaling (see Eq. 2) and including additional physics elements which are responsible for the high level of scatter in the database.

(c) A modification of the scaling laws of energy confinement based on the recognition of the fact that the dominant physics of the plasma core and edge are different.

(d) An extension of the operation of the $2\omega_{CT}$-heating scheme to reactor-like densities together with the issues such as the effect of antenna phasing on the heating efficiency and ELM-resistant antenna-plasma matching techniques for maintaining good coupling during strong ELM activity.

ACKNOWLEDGEMENTS.

The authors acknowledge warmly the discussions with the JET Scientific Council which identified several topics addressed in the experiments. They would like to thank Dr J. Strachan for discussion and liaising with the TFTR team to clarify TFTR D-T results. The authors also wish to thank Dr V. Bhatnagar for the input and editing of the manuscript.

REFERENCES

[1] JET TEAM (presented by M. Keilhacker), in Plasma Physics and Controlled Fusion Research (Proc.14th Int. Conf. Wurzburg, 1992), vol.1, IAEA, Vienna (1992) 15.

[2] HAWRYLUK, R.J. et. al., in Plasma Physics and Controlled Fusion Research (Proc.15th Int. Conf. Seville, 1994), vol.1, IAEA, Vienna (1994) 11.

[3] JET TEAM, Nucl. Fusion 32 (1992) 187.

[4] McGUIRE, K. M. et al., in Fusion Energy (Proc.16th Int. Conf. Montreal, 1996), vol.1, IAEA, Vienna (1997) 19.

[5] HAWRYLUK, R.J., Rev. of Mod. Physics 70 (1998) 537.

[6] KEILHACKER, M. et. al., Report JET-P(98)30, JET Joint Undertaking, Abingdon (UK) 1997; to be published in Nucl. Fusion.

[7] JACQUINOT, J. et. al., Report JET-P(98)31, JET Joint Undertaking, Abingdon (UK) 1997; to be published in Nucl. Fusion.

[8] AYMAR, R., et al., ITER JOINT CENTRAL TEAM, HOME TEAMS, in Fusion Energy (Proc.16th Int. Conf. Montreal, 1996), vol.1, IAEA, Vienna (1997) 3.

[9] SABBAGH, S.A. et al., in Fusion Energy (Proc.16th Int. Conf. Montreal, 1996), vol.1, IAEA, Vienna (1997) 921.
[10] GORMEZANO, C. et al., Phys. Rev. Lett. 80 (1998) 554.
[11] LEVINTON, F.M. et.al., in Fusion Energy (Proc.16th Int. Conf. Montreal, 1996), vol.1, IAEA, Vienna (1997) 211.
[12] TAYLOR, G., et al., Phys. Rev. Lett. 76 (1996) 2722.
[13] THOMAS, P.R., et al., Phys. Rev. Lett. 80 (1998) 558.
[14] NAZIKIAN, R. et.al., Phys. Rev. Lett. 78 (1997) 2976.
[15] WU, G. and VAN DAM, J., Phys. Fluids B 1 (1989) 1949.
[16] RIGHI, E. et al., submitted for publication in Nucl. Fusion special issue.
[17] SCOTT, S.D., et.al., in Fusion Energy (Proc.16th Int. Conf. Montreal, 1996), vol.1, IAEA, Vienna (1997) 573.
[18] CORDEY, J.G. et al., submitted for publication in Nucl. Fusion special issue.
[19] BHATNAGAR, V.P., LINGERTAT, J. et al, submitted for publication in Nucl. Fusion special issue.
[20] SAIBENE, G. et al, to be submitted for publication in Nucl. Fusion special issue.
[21] WILSON, J.R., et. al, Phys. Rev. Lett. 75 (1995) 842.
[22] START, D.F.H. et al, Phys. Rev. Lett. 80 (1998) 468.
[23] ERIKSSON, L-G. et al, submitted for publication in Nucl. Fusion special issue.
[24] LASSER, R. et al., Proc. Workshop on Tritium Experiments in Large Tokamaks: Applications to ITER, Princeton Plasma Physics Laboratory, March 1998.
[25] ROLFE, A., in Proc. of the 19th Symp. on Fusion Technology, Lisbon 1996, published by Elsevier (1997) 91.
[26] JET TEAM, Annual Report 1997, JET Joint Undertaking, Abingdon (UK).
[27] GRISHAM, L. et al., Nucl. Instrum. Methods Phys. Res. B 99 (1995) 353.
[28] STORK, D., Fusion Engineering and Design, 14 (1991) 111.
[29] KAYE, A. et al., Fusion Engineering and Design 24 (1994) 1.
[30] SCHILLING, G. in Proc. 10th Topical Conf. on RF Power in Plasmas, Boston, AIP Conf. Proc. 289 (1993) 3.
[31] JET TEAM (presented by J. Jacquinot), Plasma Phys. Contr. Fusion, 33 (1991) 1657.
[32] ORLINSKIJ, D.V. , MAGYAR, G., Nucl. Fusion 28 (1988) 611.
[33] MORGAN, P. D. et al., Report JET-R(97)08, JET Joint Undertaking, Abingdon (UK) 1997.
[34] WAGNER, F. et al., Phys. Rev. Lett. 49 (1982) 1408.
[35] JONES, T.T.C., JET TEAM, Report JET-P(97)05, JET Joint Undertaking, Abingdon (UK) 1997.
[36] NAVE, M.F.F. et. al., Nucl. Fusion, 37 (1997) 809.
[37] HUGON, M. et al., Nucl. Fusion 36 (1992) 33.

[38] FUJITA, T. et al., in Fusion Energy (Proc.16th Int. Conf. Montreal, 1996), vol.1, IAEA, Vienna (1997) 227.
[39] STRACHAN, J. D., et al., Phys. Rev. Lett. 58 (1987) 1004.
[40] KOTSCHENREUTHER, M., et. al., Phys. Plasmas 2 (1995) 2381.
[41] NAVRATIL, G., et. al., in Plasma Physics and Controlled Fusion Research (Proc.13th Int. Conf. Washington, 1990), vol.1, IAEA, Vienna (1990) 209.
[42] MESSIAEN, A.M., et. al., Nucl. Fusion 37 (1994) 825.
[43] ONGENA, G., et.al., in Proc. 25th EPS conf. on Plasma Physics, Prague, 1998, to be published.
[44] KADOMTSEV, B. B., in Tokamak Plasma: A complex Physical System, Plasma Physics Series, IOP Publishing, Bristol and Philadelphia (1992) 108.
[45] JONES, T.T.C., et. al., submitted for publication in Nucl. Fusion special issue.
[46] GOLDSTON, R., et. al., J. Comput. Phys. 43 (1981) 61.
[47] HORTON, L., et. al., to be submitted for publication in Nucl. Fusion special issue.
[48] ITER CONFINEMENT DATABASE AND MODELLING WORKING GROUP (Presented by J.G. CORDEY), Plasma Physics Controlled Fusion 39 supplement 12B (1997) B115.
[49] HUYSMAN, G. et. al., in Proc. 17th SOFE conf. San Diego, 1997, to be published.
[50] COTTRELL, G. et al., Report JET-P(97)53, JET Joint Undertaking, Abingdon (U.K).
[51] BELIKOV, V.S. et al., Nucl. Fusion, 35 (1995) 207.
[52] WONG, K.L., et. al., Phys. Rev Lett., 66 (1991) 1874.
[53] HEIDBRINK, W. W., et.al., Nucl. Fusion, 31 (1991) 1635.
[54] WONG, K. L., et. al., Plasma Phys Control. Fusion, 36 (1994) 879.
[55] FASOLI, A., et. al., Plasma Phys Control. Fusion, 39 (1997) B287.
[56] ALI-ARSHAD, S., et. al., Plasma Phys Control. Fusion, 37 (1995) 715.
[57] KIMURA, H., et. al., Phys. Lett. A 199 (1995) 86.
[58] WONG, K.L., et al, Phys. Rev. Lett. 76 (1996) 2286.
[59] SHARAPOV, S. E., et. al., submitted for publication to Nucl. Fusion
[60] BORBA, D., et al., Report JET-P(96)35, JET Joint Undertaking, Abingdon (UK) 1996.
[61] H-MODE DATABASE WORKING GROUP (presented by T. TIKIZUKA), in Fusion Energy (Proc.16th Int. Conf. Montreal, 1996), vol.2, IAEA, Vienna (1997) 795.
[62] ZOHM, H., Plasma Physics Controlled Fusion 38 (1996) 105.
[63] H-MODE DATABASE WORKING GROUP, in Controlled Fusion and Plasma Physics (Proc. 20th Eur. Conf, Lisbon) vol.17C, Part I, European Physical Society, Geneva (1993) 15.
[64] WAGNER, F., et.al., in Controlled Fusion and Plasma Heating (Proc. 17th Eur. Conf., Amsterdam, 1990), vol. 14B, Part I, European Physical Society, Geneva (1990) 58.
[65] SCHISSEL, D.P., et. al., Nucl Fusion 29 (1989) 185.

[66] KIKUCHI, M., et.al., in Plasma Physics and Controlled Fusion Research (Proc.14th Int. Conf. Wurzburg, 1992), vol.1, IAEA, Vienna (1993) 189.
[67] TIBONE, F., et. al., Nucl. Fusion 33 (1993) 1319.
[68] H-MODE DATABASE WORKING GROUP, in Controlled Fusion and Plasma Physics (Proc. 20th Eur. Conf, Lisbon, 1993), vol.17C, Part I, European Physical Society, Geneva (1993) 15.
[69] PETTY, C.C., LUCE, T.C., in Controlled Fusion and Plasma Physics (Proc. 24th Eur. Conf, Berchtesgaden, 1997), vol.21A, Part III, European Physical Society, Geneva (1997) 1085.
[70] JACQUINOT, J., JET TEAM, to be published in Nucl Fusion.
[71] CONWAY, G., et. al., in Proc. 25th EPS conf. on Plasma Physics, Prague, 1998, to be published.
[72] PARAIL, V., Private Communication, 1998.
[73] BHATNAGAR, V.P. et al., in Controlled Fusion and Plasma Physics (Proc. 24th Eur. Conf, Berchtesgaden, 1997), vol.21A, Part I, European Physical Society, Geneva (1997) 77.
[74] GREENWALD, M., et al., Nucl Fusion 28 (1988) 2199.
[75] EFTHIMION, P., et al, Phys. Rev. Lett. 75 (1995) 85.
[76] ZASTROW, K.D., et al., to be submitted for publication in Nucl. Fusion special issue.
[77] BHATNAGAR, V.P. et al., in RF Heating and Current Drive of Fusion Devices (Proc. 2nd Europhysics Topical Conf, Brussels, 1998), vol.22A, European Physical Society, Geneva (1998) 29.
[78] JET TEAM (Presented by JACQUINOT, J.), in Controlled Fusion and Plasma Physics (Proc. 24th Eur. Conf, Berchtesgaden, 1997), vol.21A, Part IV, European Physical Society, Geneva (1997) 1865.
[79] ITER CENTRAL TEAM, Final Design Report, International Thermonuclear Experimental Reactor Engineering Design Activity, San Diego Joint Work Site, La Jolla, California, 1997 (unpublished).